Abstracts of the Papers Published by the Staff Members of the Institute from July, 1974 to June, 1975

Nuclear Chemistry

Equations of State of Atoms for the Thomas-Fermi Theory (Applications for Atoms under a High Pressure). H. Mazaki. *Bull. Inst. Chem. Res., Kyoto Univ.,* **52**, 681 (1974).—The most simple model of atoms is a spherical atom in which the charge due to electrons is uniformly distributed. In the second model, the potential in an atom is expressed, instead of a uniform distribution, as a function of distance from the central nucleus concerned. In this case, by introducing a non-dimensional statistical potential, quantitative estimates of atomic behavior can be approximately made. This is called the Thomas-Fermi (TF) method. This method is much simpler than the self-consistent field method, but in some cases, at least for the ground state of atoms, the TF method is useful without critical-loss of accuracy. The principle of the TF method is reviewed as well as applications of the method for atoms compressed under a high pressure.

A Double Ionization Chamber for the Differential Method. H. Mazaki, E. Yoshioka, and S. Kakiuchi. *Bull. Inst. Chem. Res., Kyoto Univ.,* **53**, 1 (1975).—A double ionization chamber for measurements of a minute difference in two radioactive sources were constructed. The characteristics of each chamber were studied for various experimental conditions. By applying the differential method with this chamber, relative changes in radioactive decay rate of a nucleus, $\Delta\lambda/\lambda$, which is usually of the order of $10^{-3}\sim 10^{-4}$ can be determined. Some discussions on the differential method are also given.

Monte Carlo Calculations of Energy Response for Low-Energy γ Rays in Sodium-Iodide Crystals. T. Mukoyama. *Bull. Inst. Chem. Res., Kyoto Univ.,* **53**, 49 (1975).—A Monte Carlo method for the determination of the response function, photofraction, and total detection efficiency of sodium-iodide crystals for low-energy γ rays is described. The calculations have been carried out for point and disc sources, and for γ-ray energies less than 3 MeV. Some results obtained in the present work have been compared with experimental data and other calculated results. The influence of the source dimension on these quantities is evaluated and the effect of electron slowing down is investigated. It is shown that the response parameters for a disc source with small radius placed at a certain distance from the detector are equal to those for a point source.

Mössbauer Spectroscopy by Scattered Electrons at 77 KK. Y. Isozumi and M. Takafuchi. *Bull. Inst. Chem. Res., Kyoto Univ.,* **53**, 63 (1975).—A simple proportional counter has been designed for effective detection of low-energy electrons accompanying Mössbauer effect of the sample cooled at liquid nitrogen temperature (77K). Pure helium gas, instead of Q gas (He+6% isobutane) usually used at room temperature, has been employed as a filling gas. Some features of the counter are described.

A New Detector Assembly for Conversion Electrons and X-rays from Mössbauer Effect. Y. Isozumi, D.-I. Lee, and I. Kâdâr. *Nucl. Instr. and Meth.,* **120**, 23 (1974).—A new detector assembly has been successfully designed for simultaneous ^{57}Fe Mössbauer measurements for both thin surface layer and inside of a sample. The assembly consists of two proportional counters combined together: One is used to detect Fe K X-rays emitted after the K-shell conversion process of the resonantly excited 14.4 keV level, while the other is used to detect electrons emitted by the conversion process and by the Auger effect after the process. By means of an electronic interface specially designed, signals from the electron counter and the X-ray counter are accumulated alternatively in different memory groups of a multichannel analyser.

Fitting of Lorentzian to Mössbauer Spectra by Non-Iterative Method. T. Mukoyama. *Nucl. Instr. and Meth.,* **126**, 153 (1975).—A method for fitting a Lorentzian function in which iterative procedures are not needed is presented. The method utilizes a linearization technique of the Lorentzian function and the standard linear least-squares fitting. The validity of the proposed method has been successfully tested against the experimental Mössbauer spectrum, and a comparison with the conventional iterative least-squares method has been made.

The Effect of Pressure on Orbital Electron Capture. T. Mukoyama and S. Shimizu. *Phys. Lett.,* **50***A*, 258 (1974).—The effect of pressure on the decay rate by electron capture has been estimated on the basis of certain simplifying assumptions. For the case of ^{7}Be the order-of-magnitude agreement is found.

***K*-Shell Internal Ionization in *K*-Capture Decay of ^{55}Fe.** T. Kitahara and S. Shimizu. *Phys. Rev C,* **11**, 920 (1975).—The energy spectrum of K electrons ejected from ^{55}Fe during K-capture decay has been measured in the energy range from 5 to 180 keV. In addition, a value of the total K-shell internal ionization probability per K capture has been estimated experimentally. The phenomenon was observed by the triple-coincidence (K-x-ejected e^{-}-K-x) experiment using a gas proportional counter for ejected electrons and two gas proportional counters for Mn K x rays. For the higher-energy region of ejected electrons, the confinement of the electrons within the sensitive volume of the electron counter was achieved by applying a magnetic field. The L-shell contributions were rejected completely by the triple-coincidence technique. A fairly good agreement between our measured spectrum and theoretical curves, recently calculated relativistically by the present authors and by Intemann, is established even in the low-energy region down to 5 keV. The total ionization probability also agrees with the theoretical predictions within experimental error.

[RADIOACTIVITY ^{55}Fe; measured energy spectrum of ejected K electrons from 5 to 180 keV and total ionization probability.]

Electron Shakeoff Accompanying Internal Conversion. T. Mukoyama and S. Shimizu. *Phys. Rev. C,* **11**, 1353 (1975).—The electron shakeoff probabilities accompanying the internal conversion process have been calculated in the sudden approximation, using screened relativistic hydrogenic wave functions. The screening constants have been determined from the relativistic self-consistent-field calculations and the presence

of a vacancy resulting from internal conversion has been taken into account. The present results indicate that relativistic effects cause an appreciable increase in the probabilities. It is also shown that the prediction of Carlson *et al.* is a good approximation to the shakeoff probability accompanying internal conversion. The calculated results have been compared with available experimental data. There is fairly good agreement between the calculated and the recently measured values. The need for new data is emphasized.

Fitting of Gaussian to Peaks by Non-Iterative Method. T. Mukoyama. *Nucl. Instr. and Meth.*, **125**, 289 (1975).—A method for fitting a Gaussian spectrum without iterative procedure is presented. The method utilizes a linearization technique of the Gaussian function and the standard linear least-squares fitting. Experimental and pseudo-experimental peaks have been used to test this method and a comparison with the conventional non-linear least-squares method has been made. The present method has the advantages of not requiring the initial estimates of Gaussian parameters, and not requiring large computer memory.

Quasi Free pp and pd Scattering on ^{4}He at 155 MeV. R. Frascaria, P.G. Roos, M. Morlet, N. Marty, V. Comparat, N. Fujiwara, and A. Willis. *Contributions to the International Conference of Three Body Problems in Nuclear and Particle Physics. Quebec August* **27–31**, 107 (1974).—The energy sharing spectra for the three body ^{4}He (p, 2p) and ^{4}He (p, pd) reactions have been obtained at $\theta_1=40.2°$ and $\theta_2=40.4°$ for the Q.F.S.pp and at $\theta_1=40°$, $\theta_2=60°$ for the Q.F.S.pd. A DWIA calculations using an Eckart form wave function to describe the proton in ^{4}He has been performed for the ^{4}He (p, 2p) recation. The distorted density probability for zero recoil momentum extracted from different energy experiments (between 65 and 590 MeV) is compared to the calculation. Reasonable agreement is obtained if the calculation is multiplied by 0.5. There seems to be a discrepancy between the 480 MeV and 590 MeV data.

Proton Induced ^{3}He Break-Up at 156 MeV. J. P. Didelez, R. Frascaria, N. Fujiwara, I. D. Goldman, E. Hourany, H. Nakamura-Yokota, F. Reide, and T. Yuasa. *Contributions to the International Conference of Three Body Problems in Nuclear and Particle Physics, Quebec August* **27–31**, 110 (1974).—The ^{3}He break-up was studied at Orsay using the 156 MeV proton beam and a liquid ^{3}He target. The shape of the (p, 2p) and (p, pn) quasi-free scattering (Q F S) spectra at $\theta_1=40°$ and $\theta_2=-44°$ are found to be almost coincide with each other for the kinematic energy of the spectator particle (or quasi-particle) less than 10 MeV. The ratio of the QFS peak cross sections divided by the free two-nucleon scattering cross section is 2.0 ± 0.1. The ^{3}He p, dp) energy-sharing spectrum at $\theta_d=40°$ and $\theta_p=-70°$ shows a peak around the minimum p–d relative energy indicating a possible p–d final state interaction.

Analytical Chemistry

Nonaqueous Liquid-Liquid Extraction. Extraction of Zinc and Cadmium from Ethylene Glycol Solution of Bromide by Trioctylphosphine Oxide. M. Matsui, T. Aoki, O. Inoue, and T. Shigematsu. *Bull. Inst. Chem. Res., Kyoto Univ.,*

52, 652 (1974).—The distribution of zinc between toluene phase containing trioctylphosphine oxide (TOPO) and nonaqueous ethylene glycol phase containing either hydrogen or alkali bromide has been investigated by using zinc-65 and cadmium-115 m. The distribution ratio, D from ethylene glycol phase reached a maximum value at about 0.1 N of hydrogen bromide for zinc and at about 0.4 N for cadmium. This shows that zinc bromide complexes are considerably more stable in ethylene glycol phase than in aqueous phase. In the zinc-hydrogen or alkali bromide-TOPO system, the complex $ZnBr_2 \cdot 2TOPO$ may occur in toluene phase, while in the cadmium-hydrogen bromide–TOPO system, such acid complexes as $HCdBr_3 \cdot \ell TOPO$ and $H_2CdBr_4 \cdot mTOPO$ are probably formed in the toluene phase. Under the conditions of the experiment, only mononuclear zinc and cadmium complexes appear to exist in the two phases.

Preparation and Characterization of Bis[-(2-pyridyl) benzimidazole] iron (II) Complexes. T. Shigematsu and Y. Sasaki. *Bull. Inst. Chem. Res., Kyoto Univ.*, **52**, 658 (1974).—Bis [2-(2-pyridyl) benzimidazole] iron (II) complexes, $Fe(PBI)_2X_2$ (X= Cl^-, Br^-, NCS^-, N_3, and CN^-), were prepared and characterized on the basis of their infrared and Mössbauer spectra. In $Fe(PBI)_2(NCS)_2$, the NCS^- groups are N-bonded. The CN^- groups of $Fe(PBI)_2(CN)_22H_2O$ are in a cis position. Except for $Fe(PBI)_2(CN)_22H_2O$, the Mössbauer parameters are in the range characteristic of a Fe^{2+} ion in a high-spin form. On the other hand, the parameters of $Fe(PBI)_2(CN)_22H_2O$ are characteristic of an iron(II) ion in a low-spin form.

Spectrophotometric Determination of Calcium with Glyoxal Bis (2-hydroxyanil)—On the Color Stability—. T. Shigematsu, M. Matsui, A. Ota, and O. Fujino. *Nippon Kagaku Kaishi,* 2226 (1974), in Japanese.—Since red calcium-glyoxal bis(2-hydroxyanil) (GHA) complex is unstable in various solvent media, several experiments have been carried out to find appropriate condition for the quantitative color development. Absorbances of the reagent blank and calcium-GHA in 50% water-25% ethanol-25% 1-butanol were measured at 0～35°C for 0～120 min. Satisfactory results were obtained when the solution, 0.02 N in sodium hydroxide, 0.01% with respect to GHA and 50% with respect to the solvent mixture of ethanol and 1-butanol (1 : 1), was kept at 0°C for 30～50 min before absorbance measurement.

Ion Selective Electrode. M. Matsui and T. Shigematsu. *Farumashia,* **10**, 745 (1974), in Japanese.—Review.

Fluorometric Analysis. T. Shigematsu, Y. Takashima, and T. Tabata. *Japan Analyst* (*Annual Revies*). **23**, 61R (1974), in Japanese.—Review.

Coprecipitation of Zinc with Hydroxyapatite. O. Fujino, M. Matsui, M. Tabushi, and T. Shigematsu. *Radioisotopes,* **24**, 7 (1975).—The distribution behavior of zinc between aqueous solution phase and hydroxyapatite was studied, where solid phase was prepared by adding hydrogenphosphate ion very slowly to an aqueous solution having calcium, trace zinc and ethylenediamine at 80°C. Apparent distribution coefficient remarkably decreased as the increase of ethylenediamine which was used as a chelating agent of zinc and a buffering agent. The true distribution coefficient, K°C, was cal-

culated by using the thermodynamic data at 80°C and its value was about $10^{5.5}$. The distribution coefficient kept constant in the range of less than 10^{-5} *M* of initial zinc concentration, while the coefficient gradually decreased as the zinc concentration increased over 10^{-5} *M*.

The Coprecipitation of Strontium with Hydroxyapatite. O. Fujino. *Bull. Chem. Soc., Japan,* **48**, 1455 (1975).—The distribution behavior of the strontium ion between hydroxyapatite and the parent solution was investigated. The hydroxyapatite was formed by the extremely slow addition of diammonium hydrogenphosphate to solutions of calcium and strontium nitrate buffered with ethylenediamine at 80°C. The precipitate yielded a typical X-ray diffraction pattern of hydroxyapatite and had a composition in which the Ca/P molar ratio was 1.67 at pH 6.80. The strontium ion was coprecipitated in the apatite, obeying the Doerner and Hoskins logarithmic distribution law. The distribution coefficient was scarcely affected by the strontium concentration on the pH value in the parent solution, and had a value of 0.26 ± 0.02 at 80°C. On the other hand, the apparent distribution coefficient was a little affected by such organic anions as acetate, citrate, lactate, glycinate, and glutamate ions. The lattice constants of the precipitates prepared in the research were measured in order to confirm the formation of the solid solutions.

Activation Analysis of Environmental Samples. T. Shigematsu. *Kagaku (Kyoto).* **30**, 78 (1975), in Japanese.—Review.

Nonaqueous Liquid-Liquid Extraction: Extraction of Zinc from Ethylene Glycol Solution of Chloride by Trioctylphosphine Oxide. M. Matsui, T. Aoki, H. Enomoto, and T. Shigematsu. *Analytical Letters.* **8**, 247 (1975),—The distribution of zinc between the toluene phase containing trioctylphosphine oxide (TOPO) and the nonaqueous ethylene glycol phase containing either hydrogen or lithium chloride has been investigated by using zinc-65. In the zinc-hydrogen or lithium-chloride-TOPO system, the complex $ZnCl_2$-2TOPO may predominantly occur in the toluene phase, and only mononuclear zinc complexes appear to exist in the two phases.

Specificity of Fluorometric Reagents—Some Fluorometric Reagents for Metals—. T. Shigematsu and Y. Nishikawa. *Saishin-no Bunsekikagaku.* **26**, 35 (1975), in Japanese.—Review.

Determination of Manganese in Natural Waters by Atomic Absorption Spectrometry with a Carbon Tube Atomizer. T. Shigematsu, M. Matsui, O. Fujino, and K. Kinoshita. *Anal. Chim. Acta,* 76, 329 (1975).—The atomic absorption spectrometry of manganese was studied with carbon tube atomizers. Various inner diameters of the carbon tubes were studied: small bores gave higher sensitivity, but large bores gave higher reproducibility. A fairly linear calibration curve was obtained in the range of $1.6 \cdot 10^{-10}$ g of manganese with injection volumes of 5 μl. The detection limit was $1.5 \cdot 10^{-11}$ g and the relative standard deviation 3.5%. In 40-fold amounts, few salts interfered, but there were considerable interferences from 400 and 4000-fold amounts. Manganese in natural waters was determined by extracting it into diisobutyl ketone as the diethyl-

dithiocarbamate; the amounts found lay in the range 0.5–33 p.p.b.

Physical Chemistry

Dielectric Relaxation of W/O Emulsions in Particular Reference to Theories of Interfacial Polarization. T. Hanai and N. Koizumi. *Bull. Inst. Chem. Res., Kyoto Univ.,* **53,** 153 (1975).—Dielectric constants and electrical conductivities of water-in-oil (W/O) emulsions were measured over a wide range of concentration and at frequencies ranging from 20 Hz to 3 MHz. The W/O emulsions showed striking dielectric relaxation due to interfacial polarization at higher frequencies above 10 kHz. Both the limiting dielectric constants at high and at low frequencies were in better agreement with Hanai's theory than with Wagner's. It was reported in our previous work that limiting dielectric constants of W/O emulsions at high frequencies were decreased remarkably with the increase in shear rate and of agitation of the specimens. No such peculiar effect was observed in the present emulsions which were stabilized by minimal use of emulsifier. It is inferred that the effects of shearing and agitating W/O emulsions on their dielectric constants as previously reported may be due to the use of excessive amount of emulsifiers which are apt to form a surface layer at the water-oil interface.

Spot Test Method Convenient for Detecting the Lipid Content in Column Chromatography. S. Morita and T. Hanai. *Bull. Inst. Chem. Res., Kyoto Univ.,* **53,** 279 (1975).—A spot test method is described as a simple and quick method of estimating lipid content in fractions eluted by column chromatography. Standard spots were prepared by spotting drops of chloroform solutions of total lipids in known concentrations on a thin layer chromatographic (TLC) plate. In the course of column separation experiment, one drop of the eluate at any time was spotted on the TLC plate, and the lipid content of the spot was readily estimated by comparison with the standard spots. The method is useful for instantaneous estimation of the lipid concentration and for control of the volume and the composition of eluents in the column chromatography.

Some Problems on Emulsions, I: A. Preparation of Emulsions and their Physico-Chemical Properties. T. Hanai. *Science of Cookery,* **6**, 173 (1973), in Japanese.—This series of lectures gives reviews on some topics on emulsions. In this first lecture, preparation of emulsions and their physico-chemical properties are described concisely. Emulsifiers in common use are several surfactants having HLB values of 3.5–9 for W/O emulsions, and those of 8–18 for O/W emulsions. Methods for emulsification are classfied as simply shaking, homogenizers, spontaneous emulsification, inversion between constituent phases, and condensation by utilizing solubility change. Physico-chemical properties are further described on particle size, emulsion type, stability, and viscosity of emulsions.

Some Problems on Emulsions, II: B. Dielectric Properties of Emulsions. T. Hanai. *Science of Cookery,* **6**, 239 (1973), in Japanese.—As an introductory part of subsequent lectures, this article gives the explanation of fundamental concepts on dielectric phenomena and the principles of measuring dielectric constant and conductivity.

Some Problems on Emulsions, III: B. Dielectric Properties of Emulsions (continued). T. Hanai. *Science of Cookery,* **7,** 30 (1974), in Japanese.—Dielectric properties of emulsions obtained experimentally are described with particular reference to differences of characteristics between O/W and O/W type. The most pronounced difference is the fact that remarkable dielectric dispersions are found for W/O emulsions, whereas O/W emulsions showed no such dielectric dispersions. These characteristics are interpreted in terms of interfacial polarization quantitatively as well as qualitatively.

Some Problems on Emulsions, IV: C. Microcapsules. T. Hanai. *Science of Cookery,* **7,** 78 (1974), in Japanese.—The article gives a concise review on utility of microcapsules. As the preparation of microcapsules on a laboratory scale, two methods are introduced: Caocervation and interfacial polycondensation. Some descriptions are given also for the characteristics of particle size and ion permeability of the microcapsules.

Some Problems on Emulsions, V: D. Surface Films and Interfacial Films. T. Hanai. *Science of Cookery,* **7,** 141, (1974), in Japanese.—A routine apparatus and the method are described of forming lipid monolayers on aqueous phases. This experiment usually yields some characteristic relations between effective molecular areas and surface pressure of the monolayers. These relations can be classified as gaseous film, liquid expanded film, liquid condensed film, and solid film, being interpreted in terms of molecular orientation and interaction among molecules in the nomolayers. In the case of water-soluble molecules with a surface active property, a cross-sectional area of the molecule can be evaluated from a relation between surface tension and concentration of the molecule in the aqueous phase.

Some Problems on Emulsions, VI: E. Underwater Black Lipid Membranes. T. Hanai. *Science of Cookery,* **7,** 198 (1974), in Japanese.—An experimental method is introduced of forming underwater black lipid membranes. Detailed explanation is given for filmforming lipids and stabilizing agents. Electrical capacitance values of the membranes are shown to be extraordinarily large as compared with thin films of highpolymer materials commercially available, leading to some estimation of the membrane thickness. Electrical resistance of the membranes is a significant measure to study the permeation of the membranes to ions. Comparisons of various physico-chemical properties are reviewed between these artificial black lipid membranes and natural biological membranes.

Remarks on the Hamon Approximation. Y. Kita and N. Koizumi. *Advances in Molecular Relaxation Processes,* **7,** 13 (1975).—The accuracy of the Hamon approximation for evaluating the dielectric loss, the relaxation time, and the relaxation intensity from transient absorption current data was discussed with regard to dielectric relaxations of the Cole-Cole, Davidson-Cole and Williams-Watts type. It was found that the Hamon approximation enables us to evaluate the relaxation intensity and the dielectric loss, at frequencies higher than the relaxation frequency, with good accuracy, regardless of the type of relaxation, but it introduces significant errors in calculations of the dielectric loss at lower frequencies and in the relaxation time, particularly in relaxations of the Davidson–Cole type and other types with a narrow distribution of relaxation times. The approxi-

mation is applicable, with fairly good accuracy, to the Cole-Cole type of relaxation with a broad distribution of relaxation times.

ESR and ENDOR Spectra of Organic Stable Free Radicals: α, α, γ, γ–Bisdiphenylene-β-phenyl Allyl and its Derivatives. K. Watanabe, J. Yamauchi, H. O. Nishiguchi, Y. Deguchi, and K. Ishizu. *Bull. Inst. Chem. Res., Kyoto Univ.,* **53,** 161 (1975).—Electron spin resonance (ESR) and electron nuclear double resonance (ENDOR) spectra of $\alpha,\alpha,\gamma,\gamma$-bisdiphenylene-$\beta$-phenyl allyl radical and its derivatives have been observed and their hyperfine splitting constants and spin density distributions have been determined. The hyperfine splittings of the protons of the aryl group attached to the β-carbon of the allyl skeleton have been first observed. At low temperatures below −85°C their allyl skeletons in toluene solutions twist unsymmetrically on either side and the activation energy of the torsional vibration of the allyl skeleton is estimated to be about 2.5 Kcal/mol.

The ESR Spectra of Michler's Ketone Anion Radicals. H. Fujita, S. Kato, J. Yamauchi, H. O. Nishiguchi, and Y. Deguchi. *Bull. Chem. Soc. Japan,* **47,** 1541 (1974). —The ESR spectra of Michler's ketone anion radicals reduced by alkali metal in solution consist of five groups of lines at 20°C, but change into three groups of lines at −50°C. The assigned hyperfine splitting constants are $A_H^o=3.22$, $A_H^m=0.43$, $A_N=0.72$, $A_H^{CH_3}=0.29$ gauss at 20°C.

The Mangetic Properties of Verdazyl Free Radicals. VI ESR Studies of Pairs and Triads of the symmetrical Triphenylverdazyl Radical in the 1,3,5–Triphenylbenzene Matrix. N. Azuma, H.O. Nishiguchi, J. Yamauchi, K. Mukai, and Y. Deguchi. *Bull. Chem. Soc. Japan,* **47,** 2369 (1974).—Single-crystal ESR studies have been carried out on symmetrical triphenylverdazyl (TPV) doped in a diamagnetic 1,3,5-triphenylbenzene (TPB) cyrstal at room temperature. There have appeared seven pairs of fine-structure absorptions in addition to the hyperfine splittings. Three out of the seven pairs have been assigned as zero-field splittings due to radical pairs, while the other three pairs have been identified as from radical triads. The six fine structure tensors have been determined through the angular variation of the resonance-field separations. The structures of the pairs and triads of TPV were discussed on the basis of the fine structure tensors, the crystal structures of TPB and TPV, and the spin distribution in the radical molecule, assuming that the unit cell of the mixed crystal with the radical concentration of less than 11.1% is identical with that of the host crystal, TPB. Within the limits of the X-ray examination, this assumption was found to be reliable. It was found that the molecular planes in each species are almost parallel to the *bc*-plane and that all the *C*-phenyl rings lie in the *c*-direction.

The Chlorine Nuclear Quadrupole Resonance in an Organic Free Radical, *p*-Cl-BDPA. T. Yoshioka, J. Yamauchi, H.O. Nishiguchi, and Y. Deguchi. *Bull. Chem. Soc. Japan,* **48,** 335 (1975).—The ^{35}Cl nuclear quadrupole resonance in a stable organic free radical, 1,3-bisdiphenylene-2-*p*-chlorophenyl-allyl, *p*-Cl-BDPA, has been measured in the temperature range from 4.2 K to 1.6 K. On lowering the temperature, the resonance line became weaker and broader, and it disappeared near the Néel tem-

perature, 3.25 K. This behavior has been interpreted in terms of the presence of a hyperfine interaction.

The Intramolecular Dynamic Behavior of Tetraaryl Allyl Radicals. K. Watanabe. *Bull. Chem. Soc. Japan,* **48,** 1732 (1974).—The electron spin resonance (ESR) and the electron nuclear double resonance (ENDOR) spectra of tetraaryl allyl radicals have been observed. A comparison of the ENDOR spectra of $\alpha,\alpha,\gamma,\gamma$-tetraphenyl allyl, α,α-diphenyl-γ, γ-dianisyl allyl, and $\alpha,\alpha,\gamma,\gamma$-tetraanisyl allyl revealed that the four aryl groups are not equivalent, but are apparently to be classified into two types with different conformations in their molecular frameworks. The molecular orbital calculations on the basis of this model have shown a fairly good agreement with the observed spectra. The temperature dependence of the ENDOR spectra at $-60\sim-110$°C were analyzed, assuming mutually different twisting angles for the allyl skeleton. The activation energy of the torsional vibration of the allyl skeleton is estimated to be about 2.5 kcal/mol. The ESR spectra of $\alpha,\alpha,\gamma,\gamma$-tetraphenyl allyl and α,α-diphenyl-γ, γ-diphenylene allyl change drastically with the temperature at around $+115$°C and show a marked line-width alternation effect. It is concluded from the results that the torsional vibration becomes vigorous with an increase in the temperature and that the allyl skeleton begins to rotate internally at high temperatures. The activation energy of the internal rotation of the allyl skeleton has been estimated to be about $15\sim20$ kcal/mol. The temperature-dependent hyperfine splitting of the methine proton has also been explained by assuming a model of the internal rotation of the allyl skeleton.

Infrared Spectra and Molecular Configurations of Liquid and Crystalline Acrylic Acids. J. Umemura and S. Hayashi. *Bull. Inst. Chem. Res., Kyoto Univ.,* **52,** 585, (1974).—Polarized infrared spectra of oriented crystals of CH_2=CHCOOH and CH_2=CHCOOD were recorded at various low temperatures. An infrared spectrum of liquid acrylic acid at room temperature was also recorded. Assignments of the observed bands were made with the aid of infrared dichroism and isotropic frequency shift.

It was found that some infrared absorption bands reduced their intensities on crystallization and disappeared on futher cooling. This phenomenon was interpreted as due to the cis-trans isomerism of acrylic acid.

Raman Spectra of Benzene, Ethyl Benzene and Dimethyl Phthalate Solubilized in Aqueous Solutions of Surface-Active Agents. T. Takenaka, K. Harada, and T. Nakanaga. *Bull. Inst. Chem. Res., Kyoto Univ.,* **53,** 173 (1975).—Raman spectral studies were made of benzene, ethyl benzene, and dimethyl phthalate solubilized in aqueous solutions of sodium laurate and of sodium lauryl sulphate. The mechanism of incorporation of the solubilizates in the micelles was discussed on the basis of changes in the half band-width and frequency of their Raman bands on solubilization. It was concluded that solubilized benzene and ethyl benzene were in the same mode of solubilization and located in the hydrocarbon interior of the micelles, whereas solubilized dimethyl phthalate was adsorbed on the surface of the micelles through the hydrogen bond.

Intermolecular Forces and State Configuration of Crystalline Benzoic

Acid. J. Umemura and S. Hayashi. *Bull. Inst. Chem. Res., Kyoto Univ.,* **53,** 180 (1975).—The energy difference between the two configurations of crystalline benzoic acid, which would be transformed into each other by the simultaneous proton transfer along two hydrogen bonds of the dimer, was evaluated by using the empirical atom-atom potentials. This calculation gives reasonable value as compared with the experimental value obtained from infrared spectroscopy, providing the useful information about the stability of the two molecular configurations. It is also apparent that the intermolecular Coulombic force plays an important role in the determination of the stable configuration.

The Origin of the Archaeological Amber in Japan—Studies by Infrared Spectra— T. Fujinaga, T. Takenaka, and T. Muraga. *J. Chem. Soc. Japan,* 1653, (1974), in Japanese.—There are many archaeological amber objects found in Europe, and some attempts have been made to determine the provenance of these ambers. In Japan, a few beads have been excavated from old tomb, but the provenances of these ambers are not known.

In the present work, the authors investigated several methods of determination of provenance of Japanese amber artifacts, using scientific techniques such as elementary analyses, infrared spectroscopy and measurement of the melting point.

In the study, the geological standard samples, offered by some museums and laboratories were used. They were collected from main amber sources such as Kuji, Choshi, Mizunami, and Kobe in Japan and Fushun in Chiba. Other samples of unknown origin were; those from Todaijiyama Old Tomb in Nara prefecture and those from Nagaike Old Tomb in Kyoto prefecture.

Each infrared spectrum of these ambers shows a characteristic pattern depending upon its provenance; our samples vary considerably in color and were obtained in different ways, but nevertheless, the spectra of amber from the same provenance show the same pattern. Therefore, the authors strongly suggest that the best means of determination of the provenance of amber artifacts is to record the full spectrum of infrared adsorption and to compare with that of standard samples.

The archaeological amber samples from Todaijiyama Old Tomb and Nagaike Old Tomb were found to have the same provenance; Kuji in Iwate prefecture.

From there results, it is concluded that there were trade links between Kinki district and Tohoku district the sixth century A.D.

The Adsorption of Ethylene Glycols and their Cyclic Compounds at the Mercury-Aqueous Solution Interface. M. Matsumoto, Y. Sakamori, K. Nishizawa, A. Watanabe, *Colloid and Polymer Science,* **252,** 478 (1974).—Differential double layer capacities were measured at the interface between mercury and aqueous solution containing ethylene glycols and their cyclic compounds, and free energies of adsorption were calculated in order to study the structure of adsorbed layers of these compounds. Free energies for cyclic compounds were higher than those of others, more than half of the free energies of cyclic compounds were in parallel and others in inclined ring. The calculation of adsorbed amounts showed that cyclic compounds were in parallel, and others in inclined, orientation on the mercury surface. It was concluded that the adsorption of cyclic compounds was governed by the interaction between intra-molecular π–

electrons and electrons of mercury surface. Free energies of adsorption per -CH_2- and -OH were calculated to be −400 to −600 cal/mole, respectively.

Infrared Spectral Studies of Hydrogen Fluoride Adsorbed on Potassium Bromide. K. Wada, T. Takenaka, S. Hayashi, and S. Takeno. *Japan. J. Appl. Phys. Suppl.* **2**, *Pt.* **2**, 109, (1974).—Infrared absorption spectra of adsorbed HF on the inner surface of KBr windows have been observed at room temperature. As the equilibrium gas pressure p over the adsorbed species is changed, different spectra are obtained for the following pressure ranges: (a) $p \gtrsim 40$, (b) $15 \lesssim p \lesssim 30$, (c) $3 \lesssim p \lesssim 11$ and (d) $p \lesssim 2$ Torr. Spectral changes between adjacent pressure ranges are sharp, and these changes occur almost reversibly with variation of the pressure. The four spectra are considered to correspond to the four phases of adsorption: (a) KF·nHF ($n \geqq 4$), (b) KF·3HF, (c) KF·2HF and (d) KF·HF.

Kinetic Study on Addition of Carbon Monoxide to Methallyl Chloride in Hydrogen Fluoride Medium under High Pressure. N. Sugita, T. Furuta, K. Kudo, and Y. Takezaki. *Nippon Kagaku Kaishi* (*J. Chem. Soc. Japan, Chemistry and Industrial Chemistry*), 1380 (1974), in Japanese.—Synthesis of β-chloropivalic acid from methallyl chloride and carbon monoxide in hydrogen fluoride medium was studied kinetically. Since tarry matter formed at increased temperature and concentration, the favorable conditions are confined to the reaction temperature below 0°C and the charge mole ratio of methallyl chloride to hydrogen fluoride less than 0.02.

For example, 94 mol% yield of β-chloropivalic acid was attained in 1.5 hr under the conditions: carbon monoxide pressure 150 atm, temperature −10°C, the charge mole ratio 0.01.

Rate equation, derived from the proposed mechanism of carbon monoxide addition to the carbonium ion formed from methally chloride in hydrogen fluoride, can explain quantitatively the effects of pressure and the charge mole ratio. The rate constants ($atm^{-1} \cdot min^{-1}$), 1.68×10^{-3} (−10°C), 5.03×10^{-4} (−20°C), 2.02×10^{-4} (−30°C), and the apparent activation energy, 14 $kcal \cdot mol^{-1}$, have been obtained.

Kinetics on Palladium Catalyzed Carbonylation of Iodobenzene under Carbon Monoxide Pressure. H. Yoshida, N. Sugita, K. Kudo, and Y. Takezaki. *Nippon Kagaku Kaishi* (*J. Chem. Soc. Japan, Chemistry and Industrial Chemistry*), 1386 (1974), in Japanese.—The carbonylation of iodobenzene has been studied kinetically in the presence of catalytic amount of palladium chloride. In the reaction of iodobenzene and carbon monoxide under pressure in a methanol solution, the addition of a sufficient amount of pyridine makes the catalyst soluble to form a homogeneous solution, and facilitates the methyl benzoate formation under mild conditions.

Based on the assumption that the reaction involves methoxy- and carbomethoxy–palladium complexes, following rate equation has been derived:

$$(CH_3O)\,PdCl(Py)_2 + CO(l) \underset{k_{-1}}{\overset{k_1}{\rightleftarrows}} (CH_3OOC)PdCl(Py)_2$$

$$(CH_3OOC)PdCl(Py)_2 + PhI \xrightarrow{k_2} PhCo_2CH_3 + PdClI(Py)_2$$

$$V = \frac{k_1 k_2 H P_{co} [PdCl_2]_0 ([PhI]_0 - [Ester])}{(1 + k_d [PdCl_2]_0 t)\{k_{-1} + k_1 H P_{co} + k_2([PhI]_0 - [Ester]\} + k_d [PdCl_2]_0}$$

where k_d is rate constant of deactivation. This equation is in reasonable agreement with the experimental results.

The rate constants and the overall activation energy have been determined to be $k_1H=8.16\times10^{-2}$ atm$^{-1}\cdot$min^{-1} (H: Henry constant of CO), $k_{-1}=0.185$ min^{-1}, $k_2=7.64$ mol$^{-1}\cdot$l$\cdot$min^{-1}, $k_d=31.7$ mol$^{-1}\cdot$l$\cdot$min^{-1} at 100°C and $E_a=20.9$ kcal$\cdot$mol^{-1}, respectively.

Kinetic Study on the Synthesis of Methyl Glycolate from Methylene Sulfate and Carbon-Monoxide under Pressure. A. Yanagase, N. Sugita, K. Kudo, and Y. Takezaki. *Nippon Kagaku Kaishi* (*J. Chem. Soc. Japan, Chemistry and Industrial Chemistry*), 583, (1974), in Japanese.—Synthesis of methyl glycolate from methylene sulfate and carbon-monoxide has been studied kinetically under pressure in 1,2-dichloroethane (EDC) solution. The rate of methyl glycolate formation is of the first order with respect to carbon-monoxide pressure and nearly of the first order to the concentration of methylene sulfate.

Under the reaction conditions studied, dimeric methylene sulfate decomposes to its monomer, formaldehyde and SO_3 in equilibrium.

Based on these results, the following mechanism has been proposed: methylen sulfate monomer reacts with carbon-monoxide to form a complex which is converted into methyl glycolate by the action of methanol outside of the reaction system.

$$[CH_2OSO_3]_2 \overset{K_1}{\rightleftarrows} 2[CH_2OSO_3] \overset{K_2}{\rightleftarrows} 2HCHO+2SO_3$$

$$[CH_2OSO_3]+CO(d) \xrightarrow{k} [CH_2(CO)OSO_3]$$

$$[CH_2(CO)OSO_3]+2CH_3OH \longrightarrow CH_2(OH)COOCH_3+CH_3OSO_3H$$

The derived rate equation is:

$$V_0=kHP_{co}\left\{\left(2+\frac{\sqrt{K_2}}{2L_0}\right)-\sqrt{\left(2+\frac{\sqrt{K_2}}{2L_0}\right)^2-4}\right\}$$

$$\frac{kHP_{co}L_0}{\sqrt{K_2}}t+\frac{1}{2}=\frac{1}{2-G}+\frac{L_0}{\sqrt{K_2}}G\left(1-\frac{1}{4+\frac{\sqrt{K_2}}{L_0}}\right)$$

H: Henry constant, P_{co}: CO pressure (kg$\cdot$cm^{-2}),
L_0: Initial charge of MS (mol)/solvent (mol),
G: Methyl glycolate (mol)/Initial charge of MS (mol),

which is reasonably in agreement with the experimental results. The equilibrium constants, rate constants, Henry constant in EDC and the overall activation energy have been determined to be $K_1=1.22\times10^{-2}$, $K_2=5.7\times10^{-3}$, $k=6.05$ min^{-1}, $H^{co}_{EDC}=6.8\times10^{-4}$ kg$^{-1}\cdot$cm^2 and $E_a=28.4$ kcal$\cdot$mol^{-1}, respectively.

In the detailed experiment by changing dielectric constant of medium, the observed rate constant has been found to fit the Kirkwood modified relation, which holds for the reaction through dipole-dipole interaction.

Isomerization of Chemically Activated Propenyl Radicals. T. Ibuki, T. Murata, and Y.Takezaki. *J. Phys. Chem.*, **78**, 2543 (1974).—The unimolecular rate constant for the isomerization of propenyl to allyl radical *via* hydrogen atom migration was measured. The propenyl radical was generated by the addition of methyl radical to acetylene, the average excess energy of which when first formed was calculated to be

~41 kcal/mol. The average rate constants for isomerization were found to be 4.04×10^7 and 8.38×10^7 sec^{-1} at 129 and 180°, respectively. The experimental data were interpreted using a four-membered, cyclic activated complex model with specific rate constants calculated according to the RRKM formulation of unimolecular reactions. The best agreement between experimental and theoretical results was found when a threshold energy of 34.5 kcal/mol was used.

The Reaction of Hydrogen Atoms with Acetylene. T. Ibuki and Y. Takezaki. *Bull. Chem. Soc. Japan,* **48,** 769 (1975).—The addition of hydrogen atoms to acetylene has been investigated at room temperature. The relative rate constant for

$$H+C_2H_4 \rightarrow C_2H_5 \quad (1)$$

$$H+C_2H_2 \rightarrow C_2H_3 \quad (2)$$

was found to be $k_1/k_2=9.99\pm0.16$. The ratios of the rate constant of disproportionation to that of combination for the same radicals and for different radicals were determined to be as follows:

$$C_2H_5+C_2H_3 \rightarrow 1-C_4H_8 \quad (4)$$

$$\rightarrow C_2H_6+C_2H_2 \quad (4a)$$

$$\rightarrow 2C_2H_4 \quad (4b)$$

$$k_{4a}/k_4=0.369$$

$$k_{4b}/k_4=0.68$$

$$C_2H_3+C_2H_3 \rightarrow 1,3-C_4H_6 \quad (5)$$

$$\rightarrow C_2H_4+C_2H_2 \quad (5a)$$

$$k_{5a}/k_5=0.087$$

Charge-Transfer Complexes of Thiopyrylium Cation with Aromatic Hydrocarbons and Olefins. Z. Yoshida, T. Sugimoto, and S. Yoneda. *Bull. Chem. Soc. Japan,* **48,** 1519 (1975).—Charge-transfer (CT) interaction of the thiopyrylium cation (**1**) with aromatic hydrocarbons and olefins has been investigated by electronic spectroscopy. It is noteworthy that **1** formed a CT complex with a monoolefin. The observed CT spectra in the **1**-olefin system showed the following remarkable contrasts compared with those in the **1**-aromatic system. 1) Although one CT absorption band was observed for the **1**-aromatic hydrocarbon CT complex, while two CT absorption bands for the **1**-olefin CT complex, and 2) the value of a in the equation of $\Delta E_{CT}=aIP_D+b$ was 1.04 for the former complex and 0.27 for the latter complex. A detailed discussion on the difference between the two CT complexes is presented.

Topotaxial Formation of an Anthracene-TCNQ (1:1) Complex in the Solid Phase. Y. Murata, T. Kobayashi, N. Uyeda, and E. Suito. *J. Cryst. Growth,* **26,** 187 (1974).—Well Oriented thin crystalline films of an anthracene-TCNQ complex were formed when thin films of TCNQ, epitaxially grown on a KCl cleavage surface, were exposed to the vapor or contacted with superimposed films of anthracene. Examination by transmission electron microscopy and electron diffraction revealed that the molecular arrangement of TCNQ in the final complex has a definite relation to that in the original epitaxial films of TCNQ. The formation was interpreted in terms of nucleation controlled by charge transfer forces and molecular diffusion.

Epitaxial Growth of an Organic Semiconductor from the Vapor Phase-TCNQ on Potassium Chloride. N. Uyeda, Y. Murata, T. Kobayashi, and E. Suito. *J. Cryst. Growth,* **26,** 267 (1974).—Epitaxial films of 7,7′, 8,8′-tetracyanoquinodimethane (TCNQ), a strong electron acceptor were formed on a KCl cleavage face by condensation from the vapor phase. Electron optical studies revealed that the films assumed two different configurations depending upon the condition of the surface treatment, although they are both composed of small crystallites of *ac*-orientation and take multiple positioning with certain regularities characteristic of the individual types. It was deduced from specific features of the mutual orientation of the deposit and substrate crystals that epitaxial nucleation is governed primarily by the oriented adsorption of TCNQ molecules on the ionic lattice of KCl and secondarily by the sporadic matching of lattice points at the interface of both crystals.

Topotactic Reactions of Thin Silver Films with Selenium. J.R. Guenter, N. Uyeda, and E. Suito. *J. Cryst. Growth,* **28,** 209 (1975).—The selenidation of thin silver films at elevated temperature was found to be topotactic reaction. The epitactic nucleation takes place at first and then the phase transformation occurs into the low temperature phase. Two or even more different orientations were detected, one of which was found to grow into extended areas. Prominent planar defects in a specific orientation were also found. Qualitative explanations were given to those growth characteristics.

Adhesion and Cohesion of Powder. M. Arakawa. *Shikizai* (*Journal of the Japan Society of Color Material*), **48,** 165 (1975), in Japanese.—Review; the fundamental concepts, methods of determining and the influence of adhesion pehnomena on powder characteristics were reviewed.

Flowing Properties of Powder—Measurements and Powder Characteristics. M. Arakawa and M. Nishino. *Zairyo* (*Journal of the Society of Materials Science, Japan*), **24,** 654 (1975), in Japanese.—The rheological properties of various powders have been measured by four different methods in order to examine the effect of particle characteristics on the flow phenomena of powder. The influence of the particle characteristics on the flow behavior of powder differs among different phenomena. Therefore, calibration is needed to obtain the apparatus constants and the correlation between the results of different methods. Some calibration data of flow characteristics of various powders have been obtained by comparing the standard glass beads powder.

Inorganic Chemistry

On the Dielectric Relaxation in Ferrites due to Electron Hopping at Low Temperatures. K. Iwauchi, N. Koizumi, M. Kiyama, and Y. Bando. *Bull. Inst. Chem. Res, Kyoto Univ.,* **52,** 596 (1974).—Dielectric dispersions were found in the powder samples of Fe_3O_4, $Mn_{1.4}Fe_{1.6}O_4$, $Mn_{0.8}Fe_{2.2}O_4$, $Zn_{0.6}Fe_{2.4}O_4$ and $Mn_{0.59}Zn_{0.33}$ $Fe_{2.08}O_4$ at temperatures from 77 to 4.2 K. The dielectric relaxations were connected with the existence of Fe^{2+} ions and the magnitudes of dielectric dispersion were roughly proportional to the amounts of Fe^{2+} ions in the samples. The activation energies obtained from

the temperature dependences of electrical conductivity were close to those obtained from dielectric relaxation. The dielectric relaxation was considered to be caused by the hopping of electron between Fe^{2+} and Fe^{3+} ions on the octahedral sites in the spinel structure.

Conditions for the Formation of Fe_3O_4 by the Air Oxidation of $Fe(OH)_2$ Suspensions. M. Kiyama. *Bull. Chem. Soc. Japan,* **47,** 1646 (1974).—The optimum conditions were studied for the formation of Fe_3O_4 by the air oxidation of $Fe(OH)_2$. The suspensions obtained by mixing NaOH and $FeSO_4$ solutions in various values of $R(=2NaOH/FeSO_4)$ were subjected to oxidation with air at various temperatures. The oxidation products were then examined by X-ray powder diffraction, chemical analysis, electron microscopic observation, and BET surface-area determination. Fe_3O_4 is formed at higher temperatures than in FeOOH. The temperature of formation becomes low as R approaches 1.0. In neutral suspensions ($R<1$), Fe_3O_4 is formed *via* green rust II or a mixture of green rust II and $Fe(OH)_2$. By further oxidation, the Fe_3O_4 formed gradually changes to γ-Fe_2O_3. A mixture of α-FeOOH and either $NaFe_3(OH)_6(SO_4)_2$ or α-Fe_2O_3 is formed as the final oxidation product. In alkaline suspensions ($R>1$), Fe_3O_4 is formed directly. The morphology and ferrous-ion content of Fe_3O_4 powder change considerably with the presence of green rust II before the formation of Fe_3O_4. It is suggested that Fe_3O_4 is formed near the surface of the particles of $Fe(OH)_2$ and green rust II by the coprecipitation of ferrous ions with ferric hydroxo-complexes.

Mössbauer and Magnetic Study on Mononuclear and Oxo-bridged Binuclear Iron (III) Complexes of 1,10-Phenanthroline and 2,2′-Bipyridine. V. K. Garg, P.G. David, T. Matsuzawa, and T. Shinjo. *Bull. Chem. Soc. Japan,* **48,** 1933 (1975). —The oxo-bridged binuclear iron(III) complexes $[L_2(NCS)Fe–O–Fe(NCS)L_2]^{2+}$ (L= 1,10-phenanthroline or 2,2′-bipyridine) were prepared recently in spite of the earlier report that they could not be prepared. The unperturbed and perturbed Mössbauer spectral and magnetic susceptibility data on these compounds are reported here and compared with those for the well characterized oxo-bridged compounds $[L_2XFe–O–FeXL_2]^{2+}$ ($X=Cl^-$, Br^-, SO_4^{2-}/2 or NO_3^-). The effect of Fe-X bond ($X=Cl^-$, Br^-, SO_4^{2-}/2, NO_3^-, or NCS^-) on the Mössbauer parameters was investigated, and the results are discussed in terms of the bonding properties of these anionic ligands. The data indicate that the electronegativity of the X ligands has no significant effect on the Mössbauer parameters. Another system, the mononuclear iron(III) complexes $[FeL_2(NCS)_2](NCS)$, investigated in this work showed no Mössbauer resonance at or above 223 K and below this temperature the unperturbed spectra exhibited a broad asymmetric singlet. Magnetic susceptibilities and magnetically perturbed Mössbauer spectra indicated that iron(III) ion in these mononuclear complexes was paramagnetic with $S=5/2$.

Antiferromagnetic Resonance of Organic Free Radical Polycrystalline 1,3-Bisdiphenylene-2-(p-Chlorophenyl)-Allyl. J. Yamauchi. *Chemistry Lett.* 1031 (1974).—The paramagnetic resonance of polycrystalline 1,3-bisdiphenylene-2-(p-chlorophenyl)-allyl can be observed in the temperature region above 3.25 K. Below the temperature the anomalous resonance absorptions, which may be the antiferromagnetic resonance, were observed. This may be the first experimental observation in organic free radicals.

Mössbauer Study of Ferromagnetic Metal Sufrace. T. Shinjo, T. Matsuzawa, T. Mizutani, and T. Takada. *Proc, 2nd Internl. Conf. on Solid Surface* 1974 *Japan. J. Appl. Phys. Suppl.*, **2**, 729 (1974).—The Mössbauer source nucleus, Co^{57}, was utilized as a microprobe for studying the magnetic properties of ferromagnetic metal surface. Carrier-free Co^{57} atoms were electrolytically deposited on a surface of iron and the Mössbauer source spectrum was taken at 4.2 K. The spectrum consisted of broadened six lines and the distribution of the hyperfine field was estimated to be 240~340 kOe (cf. the bulk value, 340 kOe). The reduction of the hyperfine field suggests that the magnetic moment in the surface has shrunk in some degree.

Chemical Transport Reaction. Y. Bando. *Kagaku (Kyoto)*, **30**, 152 (1974) in Japanese.—Review.

Topotactic Reaction of Ferrite. T. Takada. *Electronic Ceramics*, **6**, 53 (1974), in Japanese.—Review.

Magnetic Heads Made of a Crystal-Oriented Spinel Ferrite. K. Kugimiya, E. Hirota, and Y. Bando. *IEEE Transactions on Magnetics, Mag* **10**, 907 (1974).—Magnetic heads made of a new ferrite material were developed. The ferrite material was a cubic Mn-Zn ferrite having a fibrous structure and a ⟨111⟩ fiber axis. The heads had merits of magnetic heads made of a polycrystalline ferrite and those of a single crystal ferrite. Especially, resistance to material crumbling was improved by a factor of more than 10 and so was the lifetime of the heads. Among the heads, one with its track surface being ∥(111) showed the most outstanding resistance to material crumbling. One with its track surface which was rubbed by magnetic tapes being ⊥(111)⊥⟨111⟩ showed an improved wear resistance and better wear resistance by ten times than the head ∥(111).

A crystal-oriented Mn-Zn ferrite had the (111) orientation of almost 100% and a porosity of about 0.1% and had magnetic properties of a polycrystalline ferrite, ie, $\mu\sim$ 15,000 at 1 kHz, Bm~3500 G and Hc~0.03 Oe.

Glass Formation in the Systems (Na_2O, K_2O or BaO)-TiO_2-Al_2O_2. T. Kokubo and M. Tashiro. *Bull. Inst. Chem. Res., Kyoto Univ.*, **52**, 633 (1974).—Glass-forming abilities of melts in the systems (R_2O or R′O)-TiO_2-Al_2O_3, where R is Li, Na or K and R′ is Ca, Sr, Ba or Pb, were examined with an ordinary crucible-melting technique, which consist of melting 15 g of raw materials in a Pt10%Ph crucible, pouring the melts onto a steel plate and pressing them into plates 1 mm thick. Clear glasses were obtained from some of the melts in the systems (Na_2O, K_2O or BaO)-TiO_2-Al_2O_3. On the basis of X-ray emission spectroscopic and infrared spectroscopic analyses, the structures of glasses obtained were inferred to be random networks consisting both of the AlO_4 tetrahedra and TiO_6 octahedra in some holes of which are occupied by Na^+, K^+ or Ba^{2+} ions. The glass-forming abilities of the examined systems were interpreted in terms of the field strengths of R and R′ ions situated in some holes of the network.

Microstructure and Properties of Fused-Cast $NaNbO_3$-$BaTiO_3$ Ceramics. S. Ito, T. Kokubo, and M. Tashiro. *Bull. Inst. Chem. Res., Kyoto Univ.*, **52**, 641 (1974).

—A fusion cast method was applied to fabricating dense polycrystalline ferroelectric $NaNbO_3$-$BaTiO_3$ ceramics which are difficult to densify by the conventional sintering method. By casting the melt of the composition $0.7NaNbO_3 \cdot 0.3BaTiO_3$ previously heated at 1500°C into a cylindrical graphite mold held at 500°C and subsequently cooling it in a laboratory atmosphere, a dense ceramic composed mainly of columnar crystals except for near the center of the mold was obtained. The crystals precipitated were the perovskite-type $NaNbO_3$-$BaTiO_3$ solid solution and their (111) or (211) planes were orientated parallel to the inner surface of the mold. Porosity and dielectric constant of the fused-cast ceramic were 3.6% and 2900, whereas those of the sintered ceramic of the same composition were 24.7% and 2200, respectively. Addition of the SiO_2 in amount of 0.03 mol ratio to the base composition of the fused-cast ceramic was found to be strongly effective in decreasing its porosity to 1.0%, without producing the appreciable detrimental effect on its dielectric constant.

Study on Crystallization of Glass by Differential Thermal Analysis. Effect of Added Oxide on Crystallization of Li_2O-SiO_2 Glasses. K. Matusita, S. Sakka, T. Maki, and M. Tashiro. *Journal of Materials Science,* **10,** 94 (1975).—Differential thermal analysis was made of 33.3 $Li_2O \cdot 66.7\ SiO_2 \cdot 3RO_n$ and $25Li_2O \cdot 75SiO_2 \cdot 3RO_n$ glasses, where RO_n is an added oxide. The exothermic temperature, T_c, due to the precipitation of lithium disilicate crystal, were plotted against the ionic radius of the cation of the added oxide. It was possible to classify the added oxides into a few groups on the basis of the valency of the cation. Within each group, the T_c increased as the ionic radius of the cation increased. It was shown that the temperature, T_n corresponding to the viscosity of 10^{10}P also increased with increasing the radius of the cation. The relation between T_c and T_n was discussed using the theory on the rates of nucleation and crystal growth. The effect of phase separation on T_c was also discussed.

Effect of Added Oxides on the Crystallization and Phase Separation of Ki_2O, $3SiO_2$ Glasses. K. Matusita, T. Maki, M. Tashiro. *Physics and Chemistry of Glasses,* **15,** 106 (1974).—Glasses of the compositions, $25Li_2O$, $75SiO_2$, $3RO_n$, where RO_n denotes various added oxides, were heated from room temperature at a rate of 5 deg C/min, and the total number of crystal nuclei formed per unit volume and the rate of crystal growth in each of the glasses were determined. The miscibility temperature, optical absorption coefficient, and viscosity of these glasses were also measured.

The miscibility temperature data were divided into two groups, one for the glasses with addition of network modifying oxides and the other for those with addition of network forming oxides. In each group, the miscibility temperature of the glass increased as the ionic field strength of the cation of the added oxides increased.

Using these results, the effect of liquid-liquid phase separation on crystallization in these glasses was investigated on the basis of crystal nucleation and growth theory.

Factors Governing the Strength of Glass-Ceramics. T. Kanbara and M. Tashiro. *Proceedings of the* 1974 *Simposium on Mechanical Behavior of Materials,* **1,** 543 (1974).—Effects of surface microstructure of glass-ceramics on their moduli of rupture were investigated, using four specimens having different thermal expansion coefficients. A glassy layer spontaneously formed on a glass-ceramic with a low thermal expansion

coefficient was found to weaken its strength markedly. The cause was attributed to tensile stress developed in the glassy layer.

Glass Formation in the Systems (R_2O or $R'O$)-Al_2O_3-(TiO_2, Nb_2O_5 or Ta_2O_5) and Optical Properties of Their Glasses. M. Tashiro, T. Kokubo, M. Nishimura, and S. Ito. *Proceedings of Tenth International Congress on Glass,* **13,** 129 (1974).—The silica-free calcium aluminate glasses transmit to longer wavelengths in the infrared than the silicates. Their refractive indices, however, are generally low. The present investigation deals with aluminate glasses having both high infrared-transmission and high refractive index. About 10 g of melts with various compositions in the ternary systems (R_2O or $R'O$)-Al_2O_3-(TiO_2, Nb_2O_5 or Ta_2O_5), where R is Li, Na, K or Cs and R′ is Ca, Sr, Ba or Pb, were poured onto a steel plate and pressed into plates approximately 1 mm thick. Fairly stable glasses were obtained from melts in the systems (Na_2O, K_2O or BaO)-Al_2O_3-TiO_2 and (K_2O or Cs_2O)-Al_2O_3-(Nb_2O_5 or Ta_2O_5). The X-ray emission and infrared spectra of these glasses suggested that the structures of the glasses were composed of random network of AlO_4 tetrahedra combined with TiO_6, NbO_6 or TaO_6 octahedra and Na^+, K^+, Cs^+ or Ba^{2+} ions being situated in some holes of the network. Most of these glasses transmitted well visible and infrared radiation of wavelengths ranging from 0.4 to 6 μm and had refractive indices as high as 1.73 to 2.00.

Organic Chemistry

Novel Synthesis of α-Amino Acids *via* Cyanosilylation of Schiff Bases. Y. Nakajima, T. Makino, H. Oda, and Y. Inouye. *Agr. Biol. Chem.,* **39,** 571 (1975).—This short communication deals with a novel regiospecific addition of trimethylsilyl cyanide to Schiff bases.

The cyanosilylation of Schiff bases with an equimolar trimethylsilyl cyanide was at first time effected at room temperature under Lewis acid (*e.g.* zinc iodide) catalysis to give the corresponding *N*-trimethyl-silylamino-nitriles in moderate yields. The resulting aminonitriles afforded, after methanolysis, hydrolysis and hydrogenation, the corresponding α-amino acids. The direct lithium aluminum hydride reduction of the cyanosilylation mixture afforded the corresponding diamines.

Terpenoids. XXX. Reactions of Enmein-Type Compounds with Lead Tetraacetate and Iodine under Irradiation. E. Fujita, I. Uchida, and T. Fujita. *Chem. Pharm. Bull.* (*Tokyo*), **22,** 1656 (1974).—As a potential biogenesis of nodosin, a minor diterpenoid from *Isodon japonicus* Hara and *I. trichocarpus* Kudo, a route from isodocarpin *via* a key-intermediate of isodoacetal-type may be assumed. So, the authors tried the reaction with lead tetraacetate and iodine under irradiation, so-called hypoiodite reaction, in hopes of the oxygen-functionalization at C-11 of isodocarpine-type compounds, but actually the reactions resulted in the formation of the 5-iodinated 5–6 cleaved 5–6 cleaved product. The details are described in this paper.

Terpenoids. XXXI. Biogenetic Classification of *Isodon* Diterpenoids. E. Fujita, M. Node, Y. Nagao, and T. Fujita. *Yakugaku Zasshi,* **94,** 788 (1974), in Japanese.

—Biogenetic consideration on the hitherto known thirty kinds of *Isodon* diterpenoids, the structures of which had been elucidated, led to their systematic classification. Discussions on their biogenesis are also presented in this report.

Terpenoids. Part XXXII. The Structure and Absolute Stereochemistry of Teucvin, A Novel Norditerpene from *Teucrium viscidum var Miquelianum.* E. Fujita, I. Uchida, and T. Fujita. *J.C.S. Perkin I,* 1547 (1974).—On the basis of an X-ray analysis on a bromine-containing derivative of teucvin, a norditerpene isolated from *Teucrium viscidum* Blume *var. Miquelianum* (Maxim.) Hara (Japanese name, "Tsurunigakusa"), and some chemical reactions on teucvin and its derivatives, the absolute structure of the natural product has been determined to be *ent*-(6R,12R)-15,16-epoxy-19--nor9,4-friedolabda-4,13(16),14-triene-18,6 : 20,12-diolactone.

5′S(3-Furyl)-2R-methyl-2′-oxo-1,2,3,4,6,7,8,8aR-octahydro-naphthalene-1-spiro-3′R-(tetrahydrofuran)-5,4R-carbolactone, teucvidin, $C_{19}H_{20}O_5$. I. Uchida, E. Fujita, Z. Taira, and K. Osaki. *Cryst. Structure Comm.,* **3,** 569 (1974).—The structure of teucvin, a nor-diterpene from *Teucrium viscidum var. Miquelianum* (Labiatae) was clarified in 1973. Fujita, Uchida, and Fujita isolated also teucvidin as a minor component from the same plant, and presumed from spectroscopic evidence that these two compounds must be diastereoisomers. Now, a crystal structure determination was carried out and the foregoing presumption was proved to be correct. The configuration and conformation of teucvin are described in this communication.

Chemistry on Diterpenoids in 1971. E. Fujita. *Bull. Inst. Chem. Res. Kyoto Univ.,* **52,** 519 (1974).—This is one of a series of annual reviews on diterpenoids chemistry by the author. Two hundred and thirty one references are collected.

Biosynthesis of Enmein and Oridonin from 15-Oxygenated Kaurenoids and 14-Deoxyoridonin. T. Fujita, S. Takao, Y. Nagao, and E. Fujita. *J.S.C. Chem. Comm.,* 666 (1974).—Incorporation of *ent*-16-kauren-15-one into enmein and of 14-deoxyoridonin into oridonin have been demonstrated by tracer experiments in *Isodon iaponicus* plants using labelled compounds. In this communication, these experimental results are reported.

The Chemistry on Diterpenoids in 1972. E. Fujita, K. Fuji, Y. Nagao, and M. Node. *Bull. Inst. Chem. Res. Kyoto Univ.,* **52,** 690 (1974).—This is one of a series of annual reviews on the chemistry on diterpenoids. In this review, 226 references are cited.

Terpenoids. XXXIII. Chemical Conversion of Enmein into Enmelol. E. Fujita and S. Nakamura. *Chem. Pharm. Bull. (Tokyo),* **23,** 858 (1975).—After several preliminary experiments, enmein has been converted into enmelol. Chemical transformation of enmein into any natural kaurene-type diterpenoid having an oxygen-function at C-1 had not been published. So, this is the first accomplishment of the conversion of this type. Since enmein had been synthesized, the conversion constituted a formal total synthesis of enmelol.

The π-π^* Circular Dichroism of $\alpha\beta$-Unsaturated γ-Lactones. I. Uchida and K. Kuriyama. *Tetrahedron Letters,* 3761 (1974).—The authors found that the chirality at the γ-carbon atom of the butenolide ring is the sign determining factor for the π-π^* CD. If the γ-carbon is asymmetrically substituted, the sign of the π-π^* Cotton effect is determined by the relative polarizability of these two substituents. In this communication, it is shown that this new empirical rule can be applied to many compounds with little exception.

An Improved Method for Methoxymethylation of Alcohols under Mild Acidic Conditions. K. Fuji, S. Nakano, and E. Fujita. *Synthesis,* 276 (1975).—This is a communication which reports an improved method for methoxymethylation. The method provides a generally applicable, high yield preparation for the O-methoxymethyl derivatives of alcohols by an acid-catalyzed acetal exchange reaction using methylal and phosphorus pentoxide in chloroform.

Studies on the Synthesis of Bisindole Alkaloids. The Synthesis, Structure and Absolute Configuration of 18′-Epi-4′-deoxo-4′-epivinblastine, 18′-Decarbomethoxy-18′-epi-4′-epivinblastine and 18′-Epi-3′,4′-dehydrovinblastine. J.P. Kutney, J. Cook, K. Fuji, A. M. Treasurywala, J. Clardy, J. Fayos, and H. Wright. *Heterocycles,* **3,** 205 (1975).—The bisindole alkaloids or "dimeric" alkaloids, vinblastine and vincristine are presently regarded as amongst the most active clinical agents for the treatment of various cancersin humans. A series of vinblastine isomers bearing the unvatural configuration at C_{18}' were synthesized for the studies on structure-activity relationships and biological screening. X-ray analyses of the synthesized compounds provided the complete structures, including absolute configuration.

Some biological activity was recognized in one of the synthesized dimeric alkaloids.

Reduction by a Model of NAD(P)H. Reduction of α-Diketones and α-Keto Alcohols by 1-Benzyl-1,4-dihydronicotinamide. Y. Ohnishi, M. Kagami, and A. Ohno. *Tetrahedron Letters,* 2437 (1975).—It was found that α-diketones and α-ketoalcohols are reduced to the corresponding alcohols by 1-benzyl-1, 4-dihydronicotinamide in the presence of magnesium ion. The reaction may be regarded as a model of biochemical reduction by means of an oxidoreductase-NAD(P)H system.

Reduction by a Model of NAD(P)H. Biomimetic Respiratory Chain Coupled with Oxidative Phosphorylation. A. Ohno, T. Kimura, S. Oka, Y. Ohnishi, and M. Kagami. *Tetrahedron Letters,* 2371 (1975).—Biomimetic respiratory chain has been constructed:

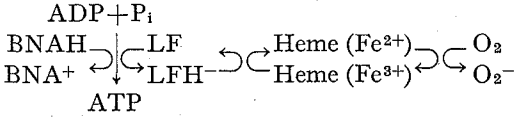

where BNAH and LF denote 1-benzyl-1, 4-dihydronicotinamide and lumiflavin, respectively. It was found that the electron-transfer from BNAH to oxygen couples with the formation of ATP from ADP and inorganic phosphate.

Reduction by a Model of NAD(P)H. Photo-Activation of NADH and its Model Compounds Toward the Reduction of Olefins. Y. Ohnishi, M. Kagami, and A. Ohno. *Chemistry Letters* 125 (1975).—Photo-excited NADH, 1-benzyl-1,4-dihydronicotinamide, or Hantzsch ester has ability to reduce a suitable olefin such as fumalic acid, maleic acid, or their esters. The reaction mechanism has been discussed.

Transannular Interactions in the Chlorination of *cis,cis*-Cyclo-octa-1,5-diene and *cis*-Cyclo-octene with $SbCl_5$. S. Uemura, A. Onoe, and M. Okano. *J. C. S. Chem. Comm.,* 210 (1975).—The chlorinations of *cis,cis*-cyclo-octa-1, 5-diene and *cis*-cyclo-octene with $SbCl_5$ in CCl_4 give *endo*- and *exo*-2-*anti*-8-dichlorobicyclo[3,2,1] octanes and *cis*- and *trnas*-1, 4-dichlorocyclo-octanes respectively in 70–80% yield.

Acetoxymercuration of Alkylphenylacetylenes. S. Uemura, H. Miyoshi, K. Sohma, and M. Okano. *J. C. S. Chem. Comm.,* 548 (1975).—Acetoxymercuration of alkylphenylacetylenes proceeds completely in a *trans* fashion to give an isomeric mixture of two vinylmercury (II) compounds, the extent of attack of Hg at the carbon α to alkyl group being increased upon increasing the carbon chain length of the alkyl group.

Acetoxythallation of Acetylenes and the Proto- and Halogenodethallation of the Products. S. Uemura, H. Tara, M. Okano, and K. Ichikawa. *Bull. Chem. Soc. Japan,* **47,** 2663 (1974).—The *trans* acetoxythallation of alkylphenylacetylene with $Tl(OAc)_3$ proceeds in acetic acid to give a mixture of two isomeric vinylthallium (III) compounds in good yields, 2-acetoxy-1-alkyl-2-phenyl- and 2-acetoxy-2-alkyl-1-phenylvinylthallium (III) diacetates [$C_6H_5C(OAc)=C(R)-Tl(OAc)_2$ (**1**) and $C_6H_5C(Tl(OAc)_2)=C(OAc)R$ (**2**)]. Protodethallation of **1** and **2** in refluxing acetic acid occurs with retention of configuration to afford $C_6H_5C(OAc)=C(R)H$ (**3**) and $C_6H_5CH=C(OAc)R$ (**4**), respectively. The reaction of **1** and **2** with $NaBH_4$ in protic solvents at pH 6–7 also gives **3** and **4** with retention of configuration, where the hydrogen for replacement of thallium group comes almost completely (>98%) from the solvent. **1** and **2** are relatively stable to water and dilute HCl, while they readily give ketones in alkaline condition. Halogeno-, cyano-, and thiocyanodethallations of **1** is conducted by reactions with the corresponding copper (II) or (I) salts in acetonitrile to give $C_6H_5C(OAc)=C(R)X$ (X=1, Br, Cl, CN, and SCN) with retention of configuration. Bromodethallation of **1** ($R=CH_3$) by bromine gives $C_6H_5C(OAc)=C(CH_3)Br$ stereospecifically in pyridine (retention), while α,α-dibromopropiophenone is obtained in CS_2 and acetonitrile.

The Reaction of Alkyl Halides with Mercuric Thiocyanate. N. Watanabe, M. Okano, and S. Uemura. *Bull. Chem. Soc. Japan,* **47,** 2745 (1974).—The reaction of secondary and tertiary alkyl halides with mercuric thiocyanate in less-polar solvents (*e.g., n*-hexane, di-*n*-butyl ether, and 1,2-dichloroethane) was found to afford predominantly N-alkylation products, alkyl isothiocyanates, in contrast to the reaction with potassium salt in DMF. Especially, from *t*-butyl bromide, α-phenethyl bromide and benzhydryl chloride, the corresponding pure isothiocyanates were obtained in good yields. A most probable reaction mechanism is suggested, based on the relative rate data, the stereochemical result of the reaction with optically active α-phenethyl bromide, and the well-known catalytic effect of silver or mercury salt in S_N1 reaction.

Alkoxythiocyanation and Alkoxyiodination of Olefins with Copper (II) Salts. A. Onoe, S. Uemura, and M. Okano. *Bull. Chem. Soc. Japan,* **47,** 2818 (1974).—A simple and convenient, method for the preparation of vicinal alkoxythiocyano- and alkoxyiodoalkanes is described. The reaction of olefins with copper (II) salts, such as chloride, bromide and sulfate, and potassium thiocyanate or iodide in alcohols readily affords the compounds in good yields. From vinyl acetates, alkyl vinyl ethers and α, β-unsaturated aldehydes, the products are obtained in the form of dialkyl acetals. The reaction mechanism is discussed.

Molybdenum (V) Chloride as a Reagent for *cis* Chlorination of Olefins. S. Uemura, A. Onoe, and M. Okano. *Bull. Chem. Soc. Japan,* **47,** 3121 (1974).—Treatment of nonconjugated olefins such as *cis*- and *trans*-2-butenes, *cis*-2-octene, and cyclohexene with $MoCl_5$ in CCl_4 gave *vic*-dichloroalkanes whose *cis*-isomer was formed predominantly, the ratio of *cis*- to *trans*-addition being 4.9-12.1, together with monochloroalkanes. Preferential formation of *exo-cis*-dichloride was observed in the case of norbornene and norbornadiene. Bromochlorination and chloroiodination of olefins, and aromatic bromination and iodination were carried out with mixtures of $MoCl_5$ and halogens. The reaction scheme for chlorination is discussed.

The Syntheses of Several N,N'-Bis (hydroxymethyl) parabanic Acid Derivatives. S. Tanimoto, R. Taniyasu, and M. Okano. *Bull. Chem. Soc. Japan,* **48,** 357 (1975).—Starting from *N,N'*-bis(hydroxymethyl) parabanic acid, the following new compounds have been synthesized: *N,N'*-bis(arylaminomethyl)parabanic acids, *N,N'*-bis (bromomethyl) parabanic acid, and *N,N'*-bis(alkoxymethyl)parabanic acids.

Aromatic Thiocyanation by a Mixture of Antimony (V) Chloride and Lead (II) Thiocyanate. S. Uemura, A. Onoe, H. Okazaki, and M. Okano. *Bull. Chem. Soc. Japan,* **48,** 619 (1975).—Alkyl- and halobenzenes give thiocyano-derivatives when treated with a mixture of $SbCl_5$ and $Pb(SCN)_2$ in CCl_4. The reaction proceeds via in situ formation of ClSCN from $SbCl_5$ and $Pb(SCN)_2$ followed by its attack on aromatic compounds catalyzed by $SbCl_5$, the reaction species being $SCN^+SbCl_6^-$.

The Reaction of N-Substituted Carbonimidic Dihalides with Grignard Reagents. The Generation of Alkyl or Aryl Halides from Grignard Reagents. S. Tanaka, M. Okano, and S. Tanimoto. *Bull. Chem. Soc. Japan,* **48,** 1862 (1975).—The reaction of *N*-alkyl- or *N*-aryl-carbonimidic dihalides with Grignard reagents afforded α-elimination products, isocyanides, rather than substitution ones. Two kinds of alkyl or aryl halides were produced concomitantly in this reaction: one kind consisted of halides generated from the Grignard reagents used, and the other, of halides the halogens of which had been derived from the dihalides. The ease of formation of these halides was found to decrease in the order: iodide>bromide>chloride, regardless of which substrate served as the source of a halogen atom. A probable reaction mechanism is proposed.

Selenocyanatodethallation in Organothallium (III) Compounds. S. Uemura, A. Toshimitsu, M. Okano, and K. Ichikawa. *Bull. Chem. Soc. Japan,* **48,** 1925 (1975).—Substitution of thallium moiety in organothallium (III) compounds by seleno-

cyanate is reported. Arylthallium (III) compounds react with KSeCN and $CuSO_4 \cdot 5H_2O$ or with $Cu(SeCN)_2$ in dioxane to give aryl selenocyanates in good yields. Alkoxythallates of styrene react smoothly with KSeCN in methanol to afford 1-alkoxy-1-phenyl-2-selenocyanatoethanes almost quantitatively. The oxyselenocyanation of terminal olefins is conducted by the *in situ* oxythallation of olefins, followed by the reaction with KSeCN.

A Convenient Preparation of p-Chloromethyl-Styrene and its Reactions. S. Tanimoto, T. Miyake, and M. Okano. *Synthetic Comm.*, **4**, 193 (1974).—A method for obtaining pure p-chloromethylstyrene from β-phenylethyl bromide *via* its p-chloromethylated compound is described. The reactions of p-chloromethyl-styrene with Mg and alcoholates, and its polymerization are also reported.

Polymer Chemistry

Separation and Characterization of Keratin Components or Merino Wool. I: A General Consideration on Methodology. H. Inagaki, H. Ando, and T. Kondo. *Bull. Inst. Chem. Res. ,Kyoto Univ.*, **52**, 597 (1974).—This paper deals with a problem of design for experimental procedures to be applied most appropriately to the disruption and dissolution of Merino wool fiber to prepare the chemically unmodified histological protein components. For the purpose, a number of works hitherto made on separation and characterization of the histological components of wool have been reviewed and assessed critically. As the result, a method using ultrasonication, designated "stepwise disintegration method", is proposed as the ideal, which consists of a series of successive experimental procedures, *i.e.*, removal of cuticular cells, disruption of decuticled fiber into cortical segments and remnant components, and separation of the former into the ortho- and paracortical segment.

Intermolecular Correlation in Light Scattering from Dilute Solutions of Block Copolymers. T. Tanaka, T. Kotaka, and H. Inagaki. *Macromolecules*, **7**, 311 (1974).—The effects of intermolecular correlation on scattered light intensities from block copolymer solutions were examined from the point of view of the distribution function theory developed by Zimm, Albrecht, and Flory and Bueche for homopolymer solutions. The theory predicts distorted Zimm plots for block copolymer solutions with solvents having nearly zero refractive index increment for one of the parent homopolymers. A larger distortion is expected, if the unmasked portion is much smaller relative to the overall dimension of a whole molecule, and if the deviation of the center of mass of the unmasked portion from the molecular center of mass is larger. Thus an AB-diblock copolymer would give a larger distortion, while a BAB-triblock copolymer a smaller distortion, if compared under the same conditions. Series of block copolymers of polystyrene and poly(methyl methacrylate) were prepared anionically. The results were found to be in agreement with the predictions of the theory. An anomalous concentration dependence of scattered light intensities found in this study is also reported.

Separation and Characterization of Keratin Components of Merino Wool. III: Removal of Cuticle by Ultrasonic Irradiation. H. Ando, Y. Nakamura, and

H. Inagaki. *Sen-i-Gakkaishi, (J. Soc. Fiber Science and Technology, Japan)* **7,** 55 (1974). —Ultrasonic irradiation under which the cuticular cells can be removed perfectly from Merino wool without giving any mechanical as well as chemical damage to the cortical entity have been investigated. An 80% aqueous solution of dichloroacetic acid have been observed. It has been presumed that liberation of cuticle is caused essentially by dissolution and/or dispersion of the cell membrane complex and intercellular materials into dichloroacetic acid.

Separation and Characterization of Keratin Components of Merino Wool. II: Reduction of Wool in Concentrated Salt Solutions. H. Ando, T. Kondo, T. Sakagushi, and H. Inagaki. *Sen-i Gakkaishi (J. Soc. Fiber Science and Technology, Japan),* **16,** 52 (1974).—Merino wool fibers have been reduced with thioglycolic acid in nearly saturated aqueous solutions of sodium chloride, in a hope that one could restrict reduction reaction to the peripheral region of fibers so that the cuticular cells are removed by a subsequent dissolution process without chemical modification of the cortical cells. Though no successful result concerning our original aim was achieved, some interesting microscopic observations were made for the cross-sections of sample fibers, which were reduced and then S-carboxymethylated. After staining of the fibers with a basic dye, their cross-sections exhibited a distinctive boundary line at the interface between the ortho- and paracortex. The condition and cause for appearance of such lines are investigated experimentally and discussed.

Separation of Isotactic and Syndiotactic Poly(methyl methacrylate) by a Competitive Adsorption Method. T. Miyamoto, S. Tomoshige, and H. Inagaki. *Polymer Journal,* **6,** 564 (1974).—A simple preparative method is presented to separate mixtures of isotactic and syndiotactic poly(methyl methacrylate) (PMMA) into components. The principle of this separation method consists in competitive adsorption of two different tactic polymers from solution onto a solid surface. Separation experiments were carried out at 25°C by using nonporous silica gel, Cab-O-Sil, as the adsorbent in chloroform, in which a stereocomplex formation between isotactic and syndiotactic PMMA does not usually occur. Some crystallizable PMMA, designated by Fox, *et al.,* as type-III polymers, were successfully separated into components on a preparative scale by using this method. The result is discussed in terms of the microstructure of these Polymer samples.

Thin-Layer Chromatographic Separations of Butadiene-Styrene Copolymers on the Basis of Composition and Molecular Weight. T. Kotaka and J.L. White. *Rubber Chem. and Technol.,* **48,** 310 (1975).—The previous article of the same title published earlier in *Macromolecules,* **7,** 107 (1974) was reproduced in this Journal because of its value to fundamental research relating to rubber and its allied substances.

Determination of Compositional Heterogeneity of Styrene-Methyl Methacrylate Block Copolymers. T. Kotaka, T. Uda, T. Tanaka, and H. Inagaki. *Makromol. Chem.,* **176,** 1273 (1975).—Determinations of compositional heterogeneity of anionically prepared block copolymers of styrene (S) and methyl methacrylate (M) were attempted by three different methods: thin-layer chromatography (TLC), cross-fractionation, and by a computer simulation method. To this end the TLC elution behavior of

diblock and triblock copolymers of SM- and MSM-type were compared with those of their statistical copolymers. A new TLC method was devised which does not require any reference samples as TLC elution standards. The compositional distributions determined by the three methods were in good agreement with one another, and found to be unexpectedly broad. The implication of such a result was discussed on the basis of the polymerization mechanism of the block copolymers.

A Note on the Chain Entanglement in Concentrated Polymer Solutions. M. Kurata, Y. Einaga, K. Osaki, and H. Odani, *Bull. Inst. Chem. Res., Kyoto Univ.,* **52,** 464 (1974).—A crude form of the relaxation spectrum for concentrated polymer solutions is presented, which is compatible, though not quantitatively, with recent experimental results of the steady-shear viscosity and compliance.

Permeation and Diffusion of Gases in Styrene-Butadiene-Styrene Block Copolymers. H. Odani, K. Taira, N. Nemoto, and M. Kurata. *Bull. Inst. Chem. Res., Kyoto Univ.,* **53,** 216 (1975).—The permeation and diffusion behavior for a series of inert gases in SBS block copolymers were studied in the temperature region from 25° to 120°C. The block copolymer samples having two different types of domain structures were prepared by careful solvent-casting and thermal treatments. The domain structures of the samples, assured by electron microscopic observation, are (a) polystyrene rods dispersed in polybutadiene matrix, and (b) alternating lamellae of styrene and butadiene components. The inert gases studied were helium, argon, krypton, xenon, and nitrogen. The permeability coefficient P was determined from the steady-state permeation rates and the diffusion coefficient D from the time-lag method. Fick's and Henry's law were accurately obeyed for all the systems over the temperature and pressure range studied. For all the systems studied the permeability coefficient P, or the diffusion coefficient D, for the copolymer samples were intermediate between those of homopolybutadiene and homopolystyrene. The coefficients P and D for the sample (a) were greater than those for the sample (b). It has been found that the observed values of P for these block copolymer samples are well explained in terms of a simple model consisted of parallel array of elements of the respective component homopolymers. From an examination of the selectivity for permeation to gases having different molecular size, however, it was suggested that permeation behavior of gases of greater molecular size through the sample (b), of lamellar-type structure, was influenced by interaction between the two different polymer phases. The trend was discussed in terms of a dependence of two impedance factors for permeation and diffusion, proposed by Michaels and Parker, on size of gas molecule. The temperature dependence of P, or D, in the temperature range 25° to 85°C was represented by the Arrhenius-type equation with constant activation energy for permeation, or diffusion. The dependence was interpreted by the fundamental relationship, suggested by Meares, between the entropy and the energy of activation. It has been inferred that, as far as the kinetic nature is concerned, the permeation and diffusion of gases in the SBS block copolymers are governed primarily by those in rubbery polybutadiene matrix.

Infinite-Dilution Viscoelastic Properties of Tobacco Mosaic Virus. N. Nemoto, J.L. Schrag, J.D. Ferry, and R.W. Fulton. *Biopolymers,* **14,** 409 (1975).—The

storage and loss shear moduli, G' and G'' ,have been measured for dilute solutions of unaggregated and aggregated tobacco mosaic virus samples in glycerol-water mixtures, by the Birnboim-Schrag multiple-lumped resonator modified for use with aqueous solvents. The frequency range was 100–5800 Hz, the concentration range $0.6–2.1\times10^{-3}$ g/ml, and the temperatures 25.0° and 37.8°C. The number-average and weight-average molecular weights of the aggregated sample were estimated as 1.4 and 2.0×10^{8}, respectively, from electron microscopy. The extrapolated intrinsic moduli $[G']$ and $[G'']$ were compared with the predictions of the Kirkwood-Auer theory for rigid rodike molecules. For the unaggregated sample, the frequency dependence of $[G']$ and $[G'']$ agreed well with the theory assuming the intrinsic viscosity to be 27 ml/g, though the asymptotic limit of $[G']M/RT$ at higher frequencies was slightly larger than the theoretical value of 3/5. For the aggregated sample, the data agreed with the theory for rigid rods as modified to account for molecular-weight distribution.

Relaxation Spectra of Concentrated Polystyrene Solutions. K. Osaki, M. Fukuda, and M. Kurata. *J. Polymer Sci, Polymer Phys. Ed.,* **13,** 775 (1975).—The relaxation modulus $G(t)$ and the stress decay after cessation of steady shear flow were measured on concentrated solutions of polystyrenes in diethyl phthalate. Ranges of concentration c and molecular weight M of the polymer were from 0.112 to 0.329 g/ml and from 1.23×10^{6} to 7.62×10^{6}, respectively. The relaxation spectrum $H(\tau)$ as calculated from $G(t)$ for the solution of very high M was found to be composed of two parts. One, at relatively short times, was a broad distribution (plateau zone) with height proportional to c^2. The second, at the long-time end, was very sensitive to concentration and gave rise to a maximum in $H(\tau)$ for very high concentrations. The behavior of $H(\tau)$ at long times was examined quantitatively by evaluating the longest relaxation time τ^0_1 and the corresponding relaxation strength G^0_1 from $G(t)$ and from the stress decay function, on the assumption of a discrete distribution of relaxation times at long times. The longest relaxation time was approximately proportional to $M^{3.5}$, even at relatively low concentrations where the zero-shear viscosity was not porportional to $M^{3.5}$. The strengths of relaxation modes with the longest few relaxation times are proportional to the third power of concentration.

Light-Scattering Studies of a Polystyrene-Poly(methyl methacrylate) Two-Block Copolymer in Mixed Solvents. H. Utiyama, K. Takenaka, M. Mizumori, M. Fukuda, Y. Tsunashima, and M. Kurata. *Macromolecules,* **7,** 515 (1974).—Light-scattering measurements were made on a two-block copolymer of polystyrene and poly(methyl methacrylate) whose molecular weight and styrene content by weight are 1.53×10^{6} and 0.38, respectively. Mixtures of toluene and furfuryl alcohol of various compositions were used as solvent. They are both good as solvent for poly(methyl methacrylate) and isorefractive as well, but the latter is a nonsolvent for polystyrene. The results show that the mean-square radius of the polystyrene subchain in the isolated block copolymer always exceeds the value for the homopolystyrene of equal molecular weight. This result confirms the view that intramolecular contacts of dissimilar units do occur. The intermolecular micelle formation set in at a solvent composition between 36.7 and 38.9 wt % of toluene. The largest micelle formed at 19.8% comprised about 72 molecules. From the shape of the particle scattering function we have concluded that the polystyrene

subchain forms a core of anisotropic shape in the beginning of aggregation but cores in larger micelles assume the shape of dense sphere. Solutions of isolated molecules and micelles both revealed an anomalous upsweep of the reciprocal scattering function at samll scattering angles but the anomaly became more pronounced for larger micelles as evidenced by a longer correlation distance. This result suggests for the micelle such a conformation as the dense polystyrene core thickly surrounded by extended chains of poly(methyl methacrylate).

Infinite-Dilution Viscoelastic Properties of Poly(*n*-hexyl isocyanate). N. Nemoto, J. L. Schrag, and J. D. Ferry. *Polymer J.*, **7**, 195 (1975).—The storage and loss shear moduli, G' and G'', have been measured for dilute solutions of three samples of poly (*n*-hexyl isocyanate) with molecular weights (M) from 0.99 to 10.0×10^5, by use of the Birnboim—Schrag multiple-lumped resonator. The frequency range was 100 to 6000 Hz, the concentration range 0.2 to 5×10^{-3} g/ml, and the temperatures 0°, 10°, 25°, and 37.8°C. Two solvents were used: Tetralin, and a Tetralin—Aroclor 1254 mixture in proportions close to 1 : 1 by weight. The molecular-weight distributions were found to be narrow from dielectric dispersion measurements. The extrapolated intrinsic moduli, $[G']$ and $[G'']$, were compared with predictions of various theories. For $M=0.99\times10^5$ in both solvents, the low-frequency behavior agreed with the Kirkwood—Auer theory for rigid rods, with the relaxation time predicted from molecular dimensions. Over the entire reduced frequency range, the data could be described closely by a hybrid relaxation spectrum of one terminal relaxation time separated by a gap from a sequence of times spaced as in the Zimm theory (as previously found for poly(γ-benzyl-L-glutamate)). For $M=3.3\times10^5$, in Tetralin, the data could be described by the Zimm theory with free draining (*i.e.*, Rouse) and finite number of submolecules $N=10$ or by the Harris—Hearst theory with free draining and a persistence length of 400 Å. For $M=3.3\times10^5$ in Tetralin—Aroclor, the molecule appeared more flexible, as shown by a fit to the Zimm theory with $N=200$ and the hydrodynamic interaction parameter $h^*=0.10$. For $M=10.0\times10^5$ in Tetralin, the data were described by the Harris—Hearst theory with slight hydrodynamic interaction and a persistence length of 63 A. The appearence of increased flexibility in the presence of chlorinated hydrocarbon solvent and the decrease in persistence length with increasing molecular weight are consistent with other physical measurements. Especially recent experiments of Yu and Rubingh, though the dynamic measurements appear to sample molecular motions which are weighted by shorter lengths than are equilibrium measurements.

Numerical Calculations of the Viscoelastic Properties of Dilute Solutions of Comb-Shaped Branched Polymers. K. Osaki, Y. Mitsuda, J.L. Schrag, and J.D. Ferry. *Trans. Soc. Rheology*, **18**, 395 (1974).—The viscoelastic properties of dilute solutions of comb-shaped branched polymers have been calculated from the bead-spring model, following the Zimm and Zimm-Kilb theories, with exact numerical evaluation of eigenvalues by the method of Lodge and Wu. Eigenvalues, relaxation times, and frequency dependence of the reduced intrinsic shear moduli $[G']_R$ and $[G'']_R$ have been obtained for various combinations of number of branch points (f) 1 to 10, beads per branch (N_b) 1 to 37, backbone beads between branches (N_s) 1 to 22, and the reduced hydro-

dynamic interaction parameter (h^*) 0 to 0.25. Since the total number of beads $(f+1)N_s+fN_s+fN_b-1$ is restricted to an unrealistically small value of 111 by computer limitations, attention is focused on the low-frequency behavior where this restriction will have the least influence. Here, the behavior is characterized by the reduced steady-state shear compliance. This quantity is quite sensitive to f when the mass backbone fraction λ is small (approaching star-shaped geometry); and for larger λ, it can detect the presence of a small number of branches.

Applicability of a Strain-Dependent Constitutive Equation of Flow Properties of a Polymer Solutions. K. Osaki, M. Fukuda, S. Ohta, and M. Kurata. *J. Soc. Pheology, Japan,* **2,** 106 (1974), in Japanese.—Applicability of a strain-dependent (S-type) constitutive equation was examined for flow properties of a polystyrene solution in diethyl phthalate. Viscoelastic quantities studied were the relaxation modulus $G(t, s)$, transient stresses at the start and cessation of steady shear flow, and the steady shear viscosity $\eta(\kappa)$. Here t is the time, s is the magnitude of shear, and κ is the rate of shear. All these quantities were measured with rheometers of cone-and-plate type. The memory function for the S-type equation was determined from experimental results on $G(t, s)$ and therefrom were calculated the stresses associated with steady shear flow. Calculated results were in good agreement with the observed over whole range of rate of shear investigated. The capability of the S-type equation was compared with that of a rate-dependent (R-type) constitutive equation on the basis of present results and some published results. It was concluded that the S-type equation is very useful in some types of flow including steady shear flow and the type of flow for measurement of relaxation modulus.

A Study on Constitutive Equations of Polymer Solutions: Application of Double-Step Stress Relaxation. M. Fukuda, K. Osaki, and M. Kurata. *J. Soc. Rheology, Japan,* **2,** 110 (1974), in Japanese.—Stress relaxation after application of double-step shear strains was measured on two concentrated solutions of polystyrene in diethyl phthalate with a cone-plate type relaxometer. The first strain s_1 was applied to the sample at time $t=-t_1$, the second strain s_2 was added at $t=0$ either in the same direction as the first or in the opposite direction, and then the shear stress was measured as a function of time t. A simple case of this type of deformation in which $s_1=-s$ and $s_2=s>0$ was found to be useful to examine the applicability of various models of single-integral type constitutive equations such as proposed by Carreau, Yamamoto, and Takahashi *et al.* No constitutive equation of this type was able to explain the experimental results quantitatively, except in the case of very small strains. The discrepancy between theoretical and experimental values of stress became more marked as the value of time interval t_1 was smaller. A new type of strain-dependent constitutive equation presented here, however, was able to represent quantitatively the stresses obtained for the type of deformation history investigated here, unless the value of t_1 was very small. This equation is of the same form as Yamamoto's, but contains the invariant of strain-tensor defined on the reference time different from that of Yamamoto's equation.

On the Pao Theory for Non-Newtonian Viscosity. K. Osaki. *J. Soc. Rheology, Japan,* **3,** 42 (1975), in Japanese.—An improved version of the Pao theory (*J.*

Polym. Sci., **61**, 413 (1962)) is given. The theory is based on a linear tensorial relation between the stress σ and the recoverable strain r^{-1} on a corotational system rigidly rotating with the material element. We discard Pao's assumption that the *ij*-element of stress is independent of *kl*-element of recoverable strain ($k \neq i$ or $l \neq j$) on the fixed orthonormal system. Instead we assume that the recoverable shear strain in steady shear flow is given by half the ratio of the principal normal stress to the shear stress. The steady shear viscosity thus obtained is very close to that of the Cox-Merz empirical law, which is applicable to many polymeric systems.

Viscosity-Molecular Weight Relationships and Unperturbed Dimensions of Linear Chain Molecules. M. Kurata, Y. Tsunashima, M. Iwama, and K. Kamada. *Polymer Handbood, 2nd edition (edited by J. Brandrup and E. H. Immergut, Wiley-Interscience Pub., John Wiley & Sons)*, **IV**, 1 1975.—About 1300 relationships between the intrinsic viscosity and molecular weight and 500 values of the unperturbed dimensions of linear chain molecules were compiled from 700 references in two forms of numerical tables. Two constants, K and a, of the Mark-Houwink-Sakurada equation, $[\eta]=K M^a$, for about 900 polymer-solvent systems are listed in the viscosity table, where the molecular weight ranges of their application and some remarks on the validity, are also indicated.

X-ray Small Angle Scattering Study on the Density of Interlamellar Regions of Drawn Polyethylene under Tensile Stress. K. Shimamura, S. Murakami, and K. Kobayashi. *Bull. Inst. Chem. Res., Kyoto Univ.*, **52**, 359 (1974).—The intensities of X-ray small angle scatterings from hot drawn high-density polyethylenes under the strains of elastic limit are measured. The changes in the intensities and the long periods by the strains lead to the conclusion that the density of polyethylene in interlamellar region is considerably lower than the melt density extrapolated to room temperature.

Broad-Line NMR Studies of Molecular Motion in Lightly Cross-Linked Polyethylene, Crystallized from the Melt under Uniaxial Compression. S.-H. Hyon, R. Kitamaru, H. Taniuchi, N. Tamura, and N. Hayakawa. *Kobunshi Ronbunshu*, **4**, 240 (1975), in Japanese.—The molecular motions in a lightly cross-linked polyethylene crystallized under various conditions involving molecular orientation are investigated by broad-line NMR. It is confirmed in a wide range of temperature that the molecular mobility in the amorphous region of the cross-linked sample crystallized from the melt under high degree of compression is almost as large as that in the isothermally well-crystallized sample of uncross-linked polymer. On the contrary, for the sample compressed to the same degree at a temperature below its melting point it is confirmed that the molecular mobility in the amorphous region is much restricted in a wide range of temperature.

Orientation of Crystallites in Lightly Cross-Linked Isotactic Polypropylene Crystallized from the Melt under Uniaxial Compression. R. Kitamaru and S.-H. Hyon. *J. Polym. Sci., Polym. Phys. Ed.*, **13**, 1085 (1975).—A lightly cross-linked polymer film was made from isotactic polypropylene by gamma-ray irradiation in an acetylene atmosphere. When the cross-linked polymer film was crystallized from the melt under uniaxial compression, a unique alignment of crystallites is found. The (040)

crystal plane is preferentially oriented parallel to the film surface at relatively low degrees of compression, and the (110) and (130) crystal planes are oriented parallel to the film surface at higher degrees of compression. The origin of these orientations, analogous to that previously found in a lightly cross-linked polyethylene, is discussed.

Biochemistry

Studies on Bacteriophage fd DNA I. A Cleavage Map of the fd Genome. M. Takanami, T. Okamoto, K. Sugimoto, and H. Sugisaki. *J. Mol. Biol.*, **95**, 21 (1975).—In order to construct a physical map of the bacteriophage fd genome, the doubly closed replicative form (RFI) DNA of phage fd was cleaved into unique fragments by four different restriction endonucleases (*Hap. Hga, HinH, and Hind*) prepared from *Haemophilus* strains *H. aphirophilus, H. gallinarum, H. influenzae* H–I and *H. influenzae* Rd, respectively. As *Hind* cleaved RFI DNA at a single site, this site was used as a reference point for mapping. *HinH* cleaved RFI DNA at three sites, *Hga* at six sites and *Hap* at I3 sites, respectively. The 5′-termini of the fragments produced by either *HinH* or *Hga* were labelled with ^{32}P in the polynucleotide kinase reaction. The labelled fragments were separated and further cleaved by other enzymes. The re-digestion products of partially digested fragments were also analysed. On the basis of these data and estimates of the size of each fragment, a cleavage map of the phage fd genome was constructed.

Studies on Bacteriophage fd DNA II. Localization of RNA Initiation Sites on the Cleavage Map of the fd Genome. T. Okamoto, K. Sugimoto, H. Sugisaki, and M. Takanami. *J. Mol. Biol.*, **95**, 33 (1975).—In an *in vitro* RNA synthesizing system, a single size of A-start RNA and three different sizes of G-start RNA are predominantly transcribed on the doubly closed replicative form (RFI) DNA of phage fd. When the RFI DNA was cleaved into three fragments (*HinH–A, HinH–B* and *HinH–C*) by a restriction endonuclease from *Haemophilus influenzae* H–I, the A-start RNA was predominantly initiated on *HinH–B* and the three G-start RNAs on *HinH-A*. RFI DNA was further cleaved into smaller pieces by two other restriction endonucleases from *H. aphirophilus* and *H. gallinarum*. Upon mixing the digests with RNA polymerase, two specific fragments derived from *HinH–A* were bound to the polymerase with GTP present. G-start RNA was efficiently initiated on the fragments isolated by this procedure. On the basis of these observations and estimates of the size of RNA formed on each fragment, the initiation sites for major RNA species were localized on the cleavage map of the phage fd genome previously constucted.

The Nucleotide Sequence of an RNA Polymerase Binding Site on Bacteriophage fd DNA. K. Sugimoto, T. Okamoto, H. Sugisaki, and M. Takanami. *Nature*, **253**, 410 (1975).—The nucleotide sequence of the RNA polymerase binding site at a promoter on fd RF DNA has been determined in comparison with the starting sequence of RNA initiated at this promoter. The RNA polymerase binding site contained the startpoint of transcription in the center and a region with twofold symmetry in the non–transcribed part.

Effect of S-(β-Aminoethyl)-L-Cysteine on Incorporation of Lysine into Protein in Bacteria. H. Tanaka and K. Soda. *Bull. Inst. Chem. Res., Kyoto Univ.*, **52**, 506 (1974).—S-(β-Aminoethyl)-L-cysteine, a sulfur analogue of lysine inhibited strongly growth of *E. coli* A-19, and weakly that of *Corynebacterium* sp. isolated from soil, but did not inhibit growth of *A. aerogenes*. In C. sp. the inhibitory effect was markedly enhanced in the presence of L-threonine. The inhibition of growth by S-(β-aminoethyl)-L-crysteine was rapidly reversed by the addition of L-lysine.

S-(β-Aminoehtyl)-L-cystein inhibited protein synthesis and the activity of lysyl-tRNA synthetase from *E. coli* and *A. aerogenes*. All the other lysine analogues tested inhibited the activity of enzyme, but S-(β-aminoethyl)-L-cysteine derivatives, S-(β-N-acetyl-aminoethyl)-L-cysteine and S-(β-aminoethyl)-α-N-acetyl-L-cysteine were not effective.

A New Assay Method of ω-Amino Acid Aminotransferase with *o*-Aminobenzaldehyde. S. Toyama, M. Yasuda, K. Miyasato, T. Hirasawa, and K. Soda. *Agr. Biol. Chem.*, **38**, 2263 (1974).—A new simple assay procedure of ω-amino acid aminotransferase with *o*-aminobenzaldehyde and glycine was established. It was observed that *o*-aminobenzaldehyde reacts with aldehydic acids, *e.g.*, glyoxylic acid and sulfoacetaldehyde to develop a yellow color with an absorption maximum at about 440 nm, but not with α-keto acids.

On the basis of the selective reactivity of *o*-aminobenzaldehyde, taurine-α-ketoglutarate aminotransferase isolated from *Achromobacter superficialis*, by which sulfoacetaldehyde is formed, can be assayed with success. The linear relationship was observed between adsorbance and the amount of enzyme or the incubation time. The results obtained by this assay method are in satisfactory agreement with those given by the conventional chromatography and ninhydrin methods. This procedure is applicable to the determination of other ω-amino acid aminotransferases.

Transamination of Hypotaurine by Taurine: α-Ketoglutarate Aminotransferase. H. Tanaka, S. Toyama, H. Tsukahara, and K. Soda. *FEBS Letters*, **45**, 111 (1974).—When taurine: α-ketoglutarate aminotransferase purified and crystallized from extracts of *Achromobacter superficialis* was incubated with hypotaurine (2-amino ethanesulfinate) and α-ketoglutarate for a long period, hypotaurine disappeared and L-glutamate was stoichiometrically formed from α-ketoglutarate. The product from hypotaurine reacted with 2,4-dinitrophenylhydrazine to form the hydrazone, which was isolated and purified, and was identified as acetaldehyde. Thus, evidence has been obtained that hypotaurine transaminates with α-ketoglutarate to yield L-glutamate, acetaldehyde and sulfite as follows.

$$NH_2\text{-}CH_2\text{-}CH_2\text{-}SO_2H + HOOC\text{-}CH_2\text{-}CH_2\text{-}CO\text{-}COOH \longrightarrow [HOC\text{-}CH_2\text{-}SO_2H] + HOOC\text{-}CH_2\text{-}CH_2\text{-}CH(NH_2)\text{-}COOH$$

The rate of enzymatic transamination of hypotaurine was about 6 times that of taurine.

Purification and Crystallization of D-Amino Acid Aminotransferase of *Bacillus sphaesicus*. K. Soda, K. Yonaha, and H. Misono. *FEBS Letters*, **46**, 359 (1974).—D-Amino acid aminotransferase of *Bacillus sphaericus* IFO 3525 was purified about 970-fold. The purification was carried out by the following step: Sonic

extraction, protamine sulfate treatment, ammonium sulfate fractionation, DEAE-cellulose column chromatography, hydroxyapatite column chromatography, and Sephadex G-150 gel filtration. The purified enzyme was crystallized by addition of ammonium sulfate. The crystals took the form of fine needles. The crystalline enzyme was shown to be homogeneous by the criteria of ultracentrifugation and disc gel electrophoresis. The sedimentation coefficient ($S^0_{20,w}$) of the enzyme was 4.30 S. The enzyme has a molecular weight of about 60,000 and consists of two subunits identical in molecular weight (30,000). The enzyme exhibits absorption maxima at 280, 330, and 415 nm, which are independent of the pH (5.5–10.0), and contains two moles of pyridoxal 5′-phosphate per mole of enzyme. D-Amino acid aminotransferase catalyzes α-transamination of various D-amino acids and α-keto acid. D-Alanine, D-α-aminobutyrate and D-glutamate, and α-ketoglutarate, pyruvate and α-ketobutyrate are the preferred amino donors and acceptors, respectively. The enzyme activity is significantly affected by both the carbonyl and sulfhydryl reagents.

Enzymatic *N*-Acetylation of Lysine Analogs: Purification and Properties of Acetyl Coenzyme A: S-(β-Aminoethyl)-L-Cysteine ω-*N*-Acetyltransferase. H. Tanaka and K. Soda. *J. Biol. Chem.*, **249**, 5285 (1974).—Acetyl-CoA: S-(β-aminoethyl)-L-cysteine ω-*N*-acetyltransferase, an enzyme catalyzing the transfer of acetyl group from acetyl-CoA to the terminal amino group of S-(β-aminoethyl)-L-cysteine, a metabolic antagonist of L-lysine, has been purified about 450-fold from the cell-free extracts of *Aerobacter aerogenes*. The purified enzyme is homogeneous by the criterion of disc gel electrophoresis and has an approximate molecular weight of 100,000. In addition to S-(β-aminoethyl)-L-cysteine, its D-enantiomer, sulfoxide, sulfone, and higher homolog, and an oxygen analog of lysine, *O*-(β-aminoethyl)-DL-serine act as acetyl acceptors. L- or D-Lysine and L- or D-ornithine also can accept an acetyl group to a certain extent, but α- or ω-*N*-acetylated derivatives of both S-(β-aminoethyl)-L-cysteine and L-lysine are not active. Acetyl-CoA is the exclusive acyl donor in the transfer reaction. The following apparent Michaelis constants were determined.: S-(β-aminoethyl)-L-cysteine, 2.1×10^{-3} M; *S*-(β-aminoethyl)-D-cysteine, 1.6×10^{-3} M; *O*-(β-aminoethyl)-DL-serine, 1.7×10^{-3} M; *S*-(β-aminoethyl)-L-homocysteine, 7.1×10^{-4} M; and acetyl-CoA, 4.5×10^{-3} M. The enzyme activity is inhibited competitively by propionyl-CoA, butyryl-CoA, and benzoyl-CoA against acetyl-CoA. *S*-(β-Aminoethyl)-α-*N*-acetyl-L-cysteine and *S*-(β-Aminoethyl)-mercaptopropionate are strong competitive inhibitors of *S*-(β-aminoethyl)-L-cysteine acetylation.

Bacterial Enzyme Catalyzing ω-*N*-Acetylation of Lysine Analogues. H. Tanaka and K. Soda. *Amino Acid and Nucleic Acid.* **30**, 88 (1974), in Japanese.—Acetyl-CoA : S-(β-aminoethyl)-L-cysteine ω-N-acetyltransferase, an enzyme catalyzing the transfer of acetyl group from acetyl-CoA to the terminal amino group of S-(β-aminoethyl)-L-cysteine, a metabolic antagonist of L-lysine, has been purified about 450-fold from the cell-free extracts of *Aerobactor aerogenes*. The purified enzyme is homogeneous by the criterion of disc gel electrophoresis, and has an approximate molecular weight of 100,000. In addition to S-(β-aminoethyl)-L-cysteine, its D-enantiomer, sulfoxide, sulfone and higher homolog, and an oxygen analog of lysine, O-(β-aminoethyl)-DL-serine

act as acetyl acceptors. L- or D-Lysine and L- or D-ornithine also can accept an acetyl group to a certain extent, but α- or ω-N-acetylated derivatives of both S-(β-aminoethyl)-L-cysteine and L-lysine are not active. Acetyl-CoA is the exclusive acyl donor in the transfer reaction. The following apparent Michaelis constants were determined; S-(β-aminoethyl)-L-cysteine, 2.1×10^{-3} M; S-(β-aminoethyl)-D-cysteine, 1.6×10^{-3} M; O-(β-aminoethyl)-DL-serine, 1.7×10^{-3} M; S-(β-aminoethyl)-L-homocysteine, 7.1×10^{-4} M; and acetyl-CoA, 4.5×10^{-3} M. The enzyme activity is inhibited competitively by propionyl-CoA, butyryl-CoA and benzoyl-CoA against acetyl-CoA. S-(β-Aminoethyl)-α-N-acetyl-L-cysteine and S-(β-aminoethyl)-mercaptopropionate are in competition with S-(β-aminoethyl)-L-cysteine to reduce potently the enzyme activity.

CDP-Choline Production from CMP and Choline by Yeasts. T. Tochikura, Y. Kariya, and A. Kimura. *Hakko Kyokaishi* (*J. Fermentation Technol.*) **52,** 637 (1974), in Japanese.—Fermentative production of CDP-choline by yeasts from CMP and choline was investigated. By use of a dried cell preparation of *Hansenula jadinii* IFO 0987, CDP-choline was produced in good yields at high levels of inorganic phosphate under the condition of glucose catabolism. CDP-choline was isolated as its sodium salt by ion exchange column chromatography, and indentified by chromatographic and physicochemical procedures. CDP-choline production by *H. jadinii* was strictly controlled by both cultivation time of cells and pH of the reaction mixture. Long time cultivation resulted in lowering the activity of both choline kinase and CDP-choline phyrophosphorylase of the cells, while the phosphorylation of CMP was not affected by long time cultivation. The optimum conditions for CDP-choline production were as follows: CMP, 20 μmoles/ml; choline, 80 μmoles/ml; glucose, 600 μmoles/ml; $MgSO_4\cdot7H_2O$, 30 μmoles/ml and dried cell preparation 100–200 mg/ml in total volume of 2 ml. Under the optimum conditions, the maximum yield of CDP-choline was more than 13 μmoles per ml.

Phosphorylation of Choline and CMP in CDP-Choline Production by Yeasts. Y. Kariya, A. Kimura, and T. Tochikura. *J. Ferment. Technol.,* **53,** 278 (1975), in Japanese.—An improved method for CDP-choline production in high yields from CMP and choline was investigated.

Fructose 1,6-diphosphate (FDP) was a more favorable energy source than glucose for CDP-choline production and for the phosphorylation of both choline and CMP under the fermentation conditions. For example, in the reaction system using FDP as an energy source, the yield of CDP-choline within a short period of incubation was much higher than that in the system using glucose.

The same results were observed in the phosphorylation of CMP and choline.

Phosphorylation of CMP did not compete with the phosphorylation of choline in their energy requirement.

Biological activities of *Hansenula jadinii* IFO 0987 with regard to high yields of CDP-choline production were studied. *H. jadinii* exhibited high activity of phospholylation of CMP to CTP under the fermentation conditions. More than 40 μmol per ml of CMP were phosphorylated within two hours incubation by 100 mg per ml of the dried cells. The organism also showed high activity of degradation of inorganic pyrophosphate. Two hundred and forty μmol of inorganic pyrophosphate were hydrolyzed by one mg

of cell per hour.

Choline kinase was purified about seventy fold from the crude extract from *H. jadinii*. Phosphorylation of choline was greatly inhibited by 10^{-3} M of CTP. By feeding a low concentration of CMP and glucose the concentration of CTP accumulated in the reaction mixture could be maintained below the level at which choline kinase was inhibited. By use of this method, more than 33 μmol per ml of CDP-choline were produced from the total concentration of 50 μmol of CMP per ml.

Tropomyosin and its Tryptic Fragments: Non-Identical Chains and Submolecular Structures. Y. Tawada, H. Ueno, S. Takahashi, and T. Ooi. *Bull. Inst. Chem. Res. Kyoto Univ.*, **52**, 672 (1974).—Tryptic fragments of tropomyosin collected by isoelectric precipitation at pH 4.6 showed three bands on SDS gel electrophoresis, two major bands corresponding to apparent molecular weights of 16,000 and 12,000, and minor one to 28,000. Those components were separated on a QAE sephadex column at pH 8.6 by increasing KCl concentration from 0.24 M to 0.5 M. For the purpose to identify the components, amino acid residues in the neighborhood of C-terminals of intact tropomyosin and the components were determined by the treatment of carboxypeptidase A. 1) C-terminals of intact tropomyosin are deduced to be isoleucine and leucine, suggesting that the two chains which constitute a coiled-coil structure are different. 2) The first component has a sequence to the C-terminal of -Met-Leu-Lys, and the last two components -Thr-Ser-Ile, which is one of the intact chains.

These results are discussed in connection with a submolecular structure of tropomyosin.

Low-Energy Structures of Two Dipeptides and their Relationship to Bend Conformations. K. Nishikawa, F. A. Momany, and H. A. Scheraga. *Macromolecules*, **7**, 797 (1974).—The low-energy conformations of two dipeptides are examined using "empirical" energy calculations and the virtual-bond method. This method enables the complete conformational space, within which bend structures occur, to be represented in tabular form. The complete conformational spaces of the dipeptides, N-acetyl-N′-methylglycyl-glycineamide and N-acetyl-N′-methyl-L-alanyl-L-alanineamide were searched systematically, and all conformations of minimum energy were found. The interaction energy between the first and second amino acid units is generally small compared to the total energy of the dipeptide at a local minimum-energy conformation. Thus, the dipeptide energy can be represented, to a first approximation, as a sum of the energies of its constituent amino acid units. Most combinations of single-residue energy minima correspond to local minima on the energy surface of the dipeptide, and the global minimum of both Gly-Gly and L-Ala-L-Ala is simply the combination of the global minima for each single residue. However, for minimum-energy bend conformations, there is a significant departure from additivity of single-residue energies. The low-energy conformation of the alanine dipeptide, which closely approximates a type II bend, does not correspond to a combination of single-residue minima. Conformations similar to a type I bend are not found to be of minimum energy for either the glycine or alanine dipeptides.

Synthesis of Sequential Polypeptides of L-Leucine and Glycine. T. Iio and S. Takahashi. *Bull. Chem. Soc. Japan*, **47**, 2720 (1974).—The following sequential poly-

peptides of L-Leucine and glycine were synthesized: $(Leu_3Gly)_n$, $(Leu_2Gly)_n$, $(LeuGly)_n$, and $(LeuGly_2)_n$. Polymerization was achieved by self-condensation of the corresponding peptide p-nitrophenyl esters. Hydrolysis of the polypeptides were carried out in 90% aqueous trifluoroacetic acid and the time course of liberation of leucine from each polymer was presented. Apparent first-order rate constants ($X10^2$), 1.93, 2.86, 2.91, and 4.4 hr^{-1} were obtained for liberation of leucine from $(Leu_3Gly)_n$, $(Leu_2Gly)_n$, $(LeuGly)_n$, and $(LeuGly_2)_n$, respectievly.

Conformations of Sequential Polypeptides of L-Leucine and Glycine in Solution. T. Iio and S. Takahashi. *Bull. Chem. Soc. Japan,* **48,** 1240 (1975).—With the aid of optical rotatory dispersion, circular dichroism, and infrared spectra, the conformations of the sequential polypeptides of L-leucine and glycine were studied and compared with the conformation of poly-L-leucine. It was shown that the polymers $(Leu)_n$, $(Leu_3Gly)_n$, $(Leu_2Gly)_n$ and $(LeuGly)_n$ could be α-helical in solution, but $(LeuGly_2)_n$ was not. The order of the stability of the α-helix of these polymers was found to be: $(Leu)_n > (Leu_3Gly)_n \sim (Leu_2Gly)_n > (LeuGly)_n > (LeuGly_2)_n$. This was attributed to interactions between side chains of L-leucines which were regularly arranged on the α-helix.

Non-Polymerizable Tropomyosin and Control of the Superprecipitation of Actomyosin. Y. Tawada H. Ohara, T. Ooi, and K. Tawada. *J. Biochem.,* **78,** 65 (1975).—Non-polymerizable tropomyosin was prepared by the digestion of several C-terminal resifues of tropomyosin with carboxypeptidase A(EC 3.4.12.2). The intrinsic viscosity and molecular weight of the non-polymerizable tropomyosin were almost the same as those of untreated tropomyosin. Like unterated tropomyosin, the non-polymerizable tropomyosin in combination with troponin repressed the superprecipitation of actomyosin in the absence of calcium, while this repression was released by addition of calcium. However the curve representing the superprecipitation rate as a function of pCa was less steep than that found with actomyosin containing untreated tropomyosin; in the former case, the rate increased to a plateau over about 2 pCa units, while in the latter case, it did so over about 1 pCa unit. These experimental results provide evidence that the "co-operation" in the regulation mechanism of skeletal muscle contraction, which is indicated by the steep curve of the contraction *versus* pCa relation, is mediated by tropomyosin-tropomyosin interaction along the thin filament.